Gremlin Plays a Key Role in the Pathogenesis of Pulmonary Hypertension

Edwina Cahill, PhD; Christine M. Costello, PhD; Simon C. Rowan, BSc; Susan Harkin; Katherine Howell, PhD; Martin O. Leonard, PhD; Mark Southwood, PhD; Eoin P. Cummins, PhD; Susan F. Fitzpatrick, BSc; Cormac T. Taylor, PhD; Nicholas W. Morrell, MD; Finian Martin, PhD; Paul McLoughlin, MB, BCh, PhD

Background—Pulmonary hypertension occurs in chronic hypoxic lung diseases, significantly worsening morbidity and mortality. The important role of altered bone morphogenetic protein (BMP) signaling in pulmonary hypertension was first suspected after the identification of heterozygous BMP receptor mutations as the underlying defect in the rare heritable form of pulmonary arterial hypertension. Subsequently, it was demonstrated that BMP signaling was also reduced in common forms of pulmonary hypertension, including hypoxic pulmonary hypertension; however, the mechanism of this reduction has not previously been elucidated.

Methods and Results—Expression of 2 BMP antagonists, gremlin 1 and gremlin 2, was higher in the lung than in other organs, and gremlin 1 was further increased in the walls of small intrapulmonary vessels of mice during the development of hypoxic pulmonary hypertension. Hypoxia stimulated gremlin secretion from human pulmonary microvascular endothelial cells in vitro, which inhibited endothelial BMP signaling and BMP-stimulated endothelial repair. Haplodeficiency of gremlin 1 augmented BMP signaling in the hypoxic mouse lung and reduced pulmonary vascular resistance by attenuating vascular remodeling. Furthermore, gremlin was increased in the walls of small intrapulmonary vessels in idiopathic pulmonary arterial hypertension and the rare heritable form of pulmonary arterial hypertension in a distribution suggesting endothelial localization.

Conclusions—These findings demonstrate a central role for increased gremlin in hypoxia-induced pulmonary vascular remodeling and the increased pulmonary vascular resistance in hypoxic pulmonary hypertension. High levels of basal gremlin expression in the lung may account for the unique vulnerability of the pulmonary circulation to heterozygous mutations of BMP type 2 receptor in pulmonary arterial hypertension. **(*Circulation*. 2012;125:920-930.)**

Key Words: bone morphogenetic proteins ■ endothelium ■ hypertension, pulmonary ■ chronic obstructive pulmonary disease ■ pulmonary vascular resistance

Pulmonary hypertension is a disease of the pulmonary circulation characterized by a sustained increase in pulmonary arterial pressure caused by an abnormally elevated pulmonary vascular resistance.[1] The development of increased vascular resistance and hypertension in hypoxia is a response unique to the pulmonary circulation; in all other organs, hypoxia causes a reduction in resistance.[2] Chronic hypoxic lung diseases are commonly complicated by pulmonary hypertension, leading to right heart failure and significantly increasing morbidity and mortality.[3] Other forms of pulmonary hypertension include those caused by right-to-left cardiac shunt, connective tissue diseases, and idiopathic pulmonary arterial hypertension (IPAH), all of which are associated with a poor prognosis.[4]

Clinical Perspective on p 930

The fundamental molecular pathogenesis of this disease process remains poorly understood. A significant breakthrough was made with the identification of heterozygous loss-of-function mutations in the bone morphogenetic protein (BMP) type 2 receptor (BMPR2) as the genetic abnormality underlying the rare heritable form of PAH (HPAH) and in a significant proportion (10% to 40%) of patients with IPAH without a family history.[5] These mutations cause attenuation of the normal cellular responses to the BMPs in the lung, where BMP2 and BMP4 play particularly important roles, resulting in pulmonary hypertension.[6–12] The BMPs bind to transmembrane receptors formed by dimerization of BMPR1

Received December 2, 2010; accepted December 28, 2011.

From the University College Dublin, School of Medicine and Medical Sciences (E.C., C.M.C., S.C.R., S.H., K.H., M.O.L., E.P.C., S.F.F., C.T.T., P.M.) and School of Biomedical and Biomolecular Sciences (F.M.), Dublin, Ireland, and University of Cambridge School of Clinical Medicine, Cambridge, UK (M.S., N.W.M.).

The online-only Data Supplement is available with this article at http://circ.ahajournals.org/lookup/suppl/doi:10.1161/CIRCULATIONAHA.111.038125/-/DC1.

Correspondence to Paul McLoughlin, MB, BCh, PhD, University College Dublin, School of Medicine and Medical Sciences, Belfield, Dublin 4, Ireland. E-mail Paul.mcloughlin@ucd.ie

and BMPR2, after which the intracellular kinase domain of BMPR2 phosphorylates its BMPR1 partner, thus initiating downstream signaling, including phosphorylation of Smad1/5/8.[13]

Subsequent studies reported that reduced BMP signaling was found in many common forms of pulmonary hypertension that are not caused by BMPR2 mutations, including hypoxic pulmonary hypertension.[9,14,15] However, it was not understood what mechanism caused reduced BMP signaling in these conditions. Additionally, it was unclear why only a small proportion (≈15% to 20%) of family members with BMPR2 mutations develop HPAH or why the vascular abnormality is restricted to the pulmonary circulation when the expression of mutant BMPR2 is ubiquitous in all vascular beds.[16]

Using a microarray screening approach, we had previously identified gremlin 1 as one of a cluster of genes whose transcription was selectively increased in hypoxic pulmonary endothelial cells in vitro but was unchanged in the endothelial cells of systemic vessels.[17] This gene was of particular interest in that it encodes for a glycoprotein that is a member of a large family of secreted BMP antagonists that modulate BMP actions.[6,12,18] Intriguingly, gremlin 1 binds with high affinity to and blocks the actions of BMP2 and BMP4, the BMPs that play central roles in the homeostasis of the normal pulmonary circulation.[6–8,12]

The aim of this study was to examine the hypothesis that pulmonary hypoxia stimulated increased gremlin 1 expression in and secretion from the vascular endothelium, inhibited endogenous BMP signaling, and thus contributed to the development of pulmonary hypertension.

Methods

Detailed methods are available in the online-only Data Supplement.

Mice

Gremlin 1 heterozygote knockout (grem1$^{+/-}$) mice and wild-type littermates were bred and genotyped as described previously.[19,20] All procedures were approved by the University College Dublin Animal Research Ethics Committee and carried out under license.

Male adult mice (age, 10–12 weeks) were exposed to hypoxic conditions in an environmental chamber (FIO_2=0.10) for periods from 3 hours to 3 weeks, and age- and weight-matched controls were maintained in normoxic conditions (FIO_2=0.21).[2,21] Then, mice were killed by exsanguination under anesthesia for isolation of tissues, which were frozen for later extraction of protein for immunoblotting and mRNA for real-time polymerase chain reaction.[17]

Immunostaining

Mouse lungs were removed postmortem and fixed, and wax-embedded sections were prepared for immunohistochemical and immunofluorescent staining as previously described.[22] Specimens from human lungs with IPAH and HPAH were obtained at the time of transplantation; control specimens were obtained from lung tissue resected during surgery for cancer at a site remote from the tumor. All patients gave informed consent.

Cell Culture

Primary human pulmonary microvascular endothelial cells (Lonza Bioscience) were cultured in hypoxic (1% O_2, 5% CO_2, and 94% N_2) or control (21% O_2, 5% CO_2, and 74% N_2) conditions for 48 hours. Scratch closure assays in endothelial monolayers were undertaken as previously described.[17]

To knock down endogenous hypoxia-inducible factor (HIF)-1α or HIF2α, cells (human microvascular endothelial cells from the lung) were transfected with HIF1α- or HIF2α-specific siRNA, respectively (10 nmol/L; Smartpool, Dharmacon), with lipofectin (Invitrogen Life Technologies). A nontargeting siRNA was used as a negative control. After transfection, cells were placed in normoxic or hypoxic (1% O_2) conditions for a further 48 hours and then lysed for RNA extraction. HIF1α, HIF2α, and gremlin 1 mRNA expression was measured by real-time polymerase chain reaction.

Assessment of Pulmonary Vascular Resistance

Pulmonary vascular resistance was assessed with an isolated ventilated lung preparation perfused at constant flow.[2,22] Afterward, the hearts were fixed for later determination of right and left ventricular weights.

Stereological Morphometry

After anesthesia, anticoagulation, and exsanguination, mouse lungs were perfused with horse blood at standard pressure (30 cm H_2O) and fixed with intratracheal glutaraldehyde (25 cm H_2O). Left lung volumes were measured, and lungs were then processed to obtain isotropic, uniform, random resin-embedded sections (1 μm) for stereological quantification of the pulmonary vasculature (Figure I in the online-only Data Supplement) by a blinded reviewer.[21]

Statistical Analyses

Normally distributed data are reported as mean±SEM, and nonnormally distributed data are presented as median±interquartile range. For normally distributed data, the statistical significance of differences between 2 group means in planned a priori comparisons was determined with the use of paired or unpaired *t* tests. For nonnormally distributed data, statistical significance was determined with the Mann-Whitney rank-sum (unpaired) or Wilcoxon signed-rank (paired) tests; *P* values were computed with the exact (permutation) method. Multiple post hoc comparisons were made with the Holms-Sidak step-down test.[23] Values of $P<0.05$ were accepted as significant.

Results

Expression of Gremlin 1 in Hypoxic Pulmonary Endothelium

In normoxic mice, gremlin 1 was expressed more highly in the lung than in a panel of other organs, including the heart, kidney, and liver (Figure 1A). On exposure to hypoxia, gremlin 1 expression increased rapidly within hours and reached a peak value during the first days of exposure, demonstrating that the increase was an early hypoxic response (Figure 1B) that had returned to baseline after 2 weeks. This period corresponds to the interval during which hypoxia-induced vascular remodeling is largely completed.[24] Interestingly, basal expression of gremlin 2, a secreted BMP antagonist that is highly homologous to gremlin 1 and binds to BMP2 and BMP4 with high affinity,[6,12] was also markedly higher in the lung than in other organs, although it was not upregulated by hypoxia (Figures IIA and IIIA in the online-only Data Supplement). Noggin and chordin, 2 other secreted BMP antagonists that inhibit BMP2 and BMP4 actions,[6,12] were not highly expressed in the lung under basal conditions and did not show hypoxia-induced changes (Figures IIB, IIC, IIIB, and IIIC in the online-only Data Supplement).

Immunohistochemical staining showed gremlin in the small intra-acinar vessels of hypoxia-exposed lungs in a distribution suggesting endothelial localization (Figure 1C and 1D), which was increased compared with normoxic lungs

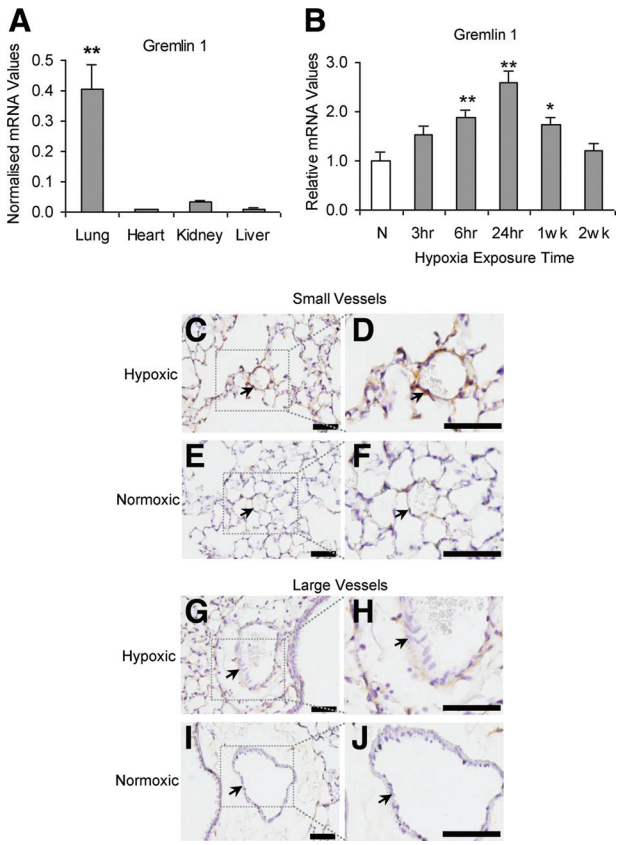

Figure 1. Gremlin is upregulated in the pulmonary vascular endothelium in hypoxic mice. **A**, High basal gremlin 1 mRNA expression in the mouse lung compared with the systemic organs (n=7). Values (mean±SE) were normalized to 18S rRNA (**$P<0.01$, significantly different from all other organs). **B**, Gremlin 1 mRNA expression (mean±SE) in mouse lungs (n=8) after hypoxic exposure from 3 hours to 2 weeks. N indicates normoxia group. Values are normalized to 18S rRNA and expressed as fold change relative to normoxic control. *$P<0.05$ and **$P<0.01$, significantly different from normoxic group. **C** through **F**, Representative images showing immunostaining (brown) of gremlin in the small intra-acinar vessels (arrows) in a hypoxic mouse (**C**) and a normoxic mouse (**E**) in a pattern compatible with endothelial localization. **D** and **F,** Higher-magnification images of vessels in **C** and **E**, respectively. No significant gremlin expression was detected in the endothelium of large extra-acinar vessels of normoxic (**G**) or hypoxic (**I**) lungs. **H** and **J**, These vessels at higher magnification (×40 objective; scale bar=50 μm).

(Figure 1E and 1F). In contrast, gremlin staining was minimal or absent in the endothelium and media of large muscularized pulmonary vessels under both normoxic (Figure 1G and 1H) and hypoxic (Figure 1I and 1J) conditions. Hypoxia also caused increased gremlin staining within the alveolar walls (Figure IVA and IVB in the online-only Data Supplement). Confocal images of immunofluorescently stained sections demonstrated gremlin labeling within the alveolar walls in a pattern that suggested expression in the capillary endothelium (Figure IVC in the online-only Data Supplement).

BMP Signaling in Hypoxic Lungs

BMP2 and BMPR2 protein levels were significantly reduced after 2 days of exposure to hypoxia (Figure 2A), whereas BMP4 and BMPR1A protein were not significantly altered. Smad1/5/8 phosphorylation was reduced, demonstrating an overall reduction in BMP-mediated cell signaling (Figure 2B and 2C). Correspondingly, expression of the BMP-regulated gene *Id1* was also reduced and remained attenuated after 2 weeks of hypoxia, in agreement with previous reports of persistently reduced BMP signaling in hypoxic lungs.[14,25]

Hypoxia Stimulates Gremlin Secretion From Human Pulmonary Microvascular Endothelial Cells, Which Blocks Endothelial BMP Signaling

Exposure of cultured human pulmonary microvascular endothelial cells to hypoxia (48 hours) caused increased gremlin 1 expression, which was abolished by siRNA-mediated knockdown of HIF2α but not by knockdown of HIF1α (Figure 3). Effective HIF1α and HIF2α knockdown was confirmed by real-time polymerase chain reaction (Figure V in the online-only Data Supplement). Because HIF-dependent gene transactivation in hypoxia results from hypoxia-induced prolyl hydroxylase inhibition, we examined the effect of a low-molecular-weight inhibitor of prolyl hydroxylases, dimethyloxalylglycine,[26,27] and found that it also caused increased gremlin expression, an action that was blocked by HIF2α knockdown (Figure VIA in the online-only Data Supplement). In contrast to the endothelial cells, gremlin 1 expression in human pulmonary artery smooth muscle cells was not altered by hypoxia (Figure VIB in the online-only Data Supplement).

Endothelial secretion of gremlin into the medium was significantly increased after hypoxic exposure (Figure 4A). Mean BMP2 concentration in the medium in hypoxia was lower than that in normoxic medium, although this difference was not significant ($P=0.07$), whereas mean BMP4 secretion was significantly increased by hypoxia (Figure 4B and 4C). The net effect of these changes was reduced BMP signaling, as demonstrated by reduced Smad1/5/8 phosphorylation and reduced *Id1* expression (Figure 4D and 4E).

Effects of Hypoxia-Induced Gremlin 1 Secretion on BMP Actions in Pulmonary Microvascular Endothelial Cells

Basal Smad1/5/8 phosphorylation was observed in the endothelial cells in normoxia in vitro, which was significantly reduced by the addition of recombinant gremlin 1 to the medium (Figure 5A and 5C and Figure VII in the online-only Data Supplement). This inhibitory action of gremlin 1 is compatible with an autocrine action of the BMP2 and BMP4 secreted by these cells under basal conditions (Figure 5A and 5C). Recombinant BMP2 stimulated a marked increase in Smad1/5/8 phosphorylation over basal conditions, an action that was blocked by recombinant gremlin 1 (Figure 5A and 5C). Cell culture medium conditioned by previous exposure to hypoxic endothelial cells (48 hours) reduced BMP2-induced Smad1/5/8 phosphorylation to basal values in a manner similar to recombinant gremlin 1 (Figure 5A and 5C), a functional activity compatible with the high gremlin concentrations that we had demonstrated in hypoxia medium (Figure 4A). Importantly, both recombinant gremlin 1 and hypoxia-conditioned medium also blocked BMP4-induced

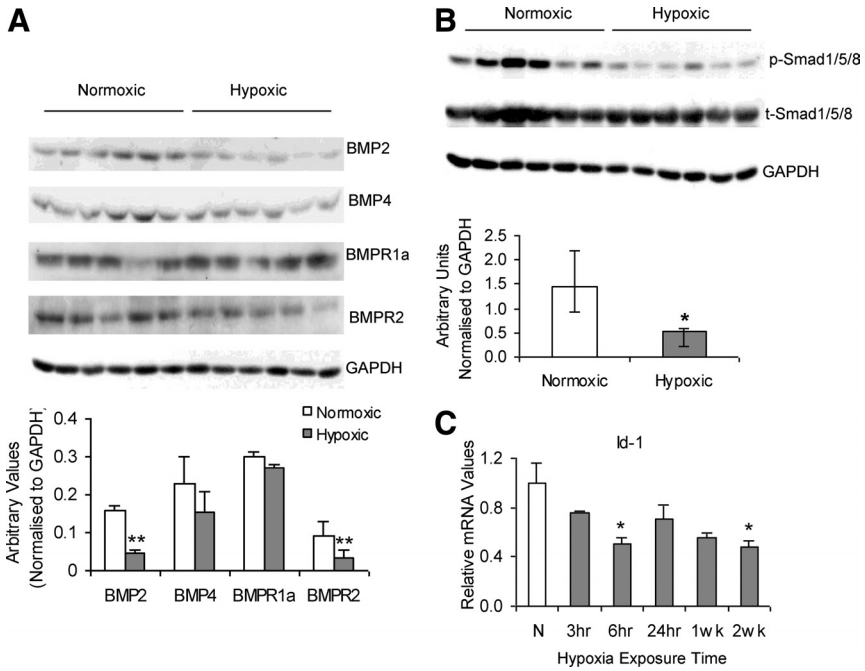

Figure 2. Bone morphometric protein (BMP) ligands and receptors (BMPRs) are altered in response to hypoxia. **A**, Western blot showing downregulation of BMP2 and BMPR2, with BMP4 and BMPR1a remaining unaltered in response to hypoxic exposure (48 hours) in mouse lungs. Densitometry (mean±SE) shows a significant reduction in BMP2 and BMPR2 in hypoxia (n=6). **B**, Western blot and densitometric analysis (median±interquartile range) showing that Smad1/5/8 phosphorylation was reduced in hypoxic conditions compared with normoxic values (n=6). **C**, The BMP target gene *Id1* was significantly downregulated (mean±SE) in hypoxic mouse lungs compared with normoxic controls (n=8). Values are normalized to 18S rRNA and expressed as fold change relative to normoxic control. *$P<0.05$ and **$P<0.01$, significantly different from normoxic values.

Smad1/5/8 phosphorylation (Figure VIII in the online-only Data Supplement).

To further examine the function of gremlin in the hypoxia-conditioned medium, we used a goat anti-gremlin antibody that antagonized the activity of recombinant gremlin 1 (Figure IX in the online-only Data Supplement). Addition of this blocking antibody to hypoxia-conditioned medium from endothelial cells abolished the inhibitory action of the medium on BMP2-induced Smad1/5/8 phosphorylation (Figure 5B and 5C), demonstrating that gremlin was the predominant antagonist of BMP2/BMP4 signaling in the hypoxic medium.

To investigate the functional effects of gremlin 1 on the pulmonary microvascular endothelial cells, we used a scratch closure assay that examines the repair and regeneration of an endothelial cell monolayer. Mean±SEM closure in vehicle-treated monolayers was (31.2±3.4%), which was not significantly changed after treatment with gremlin 1 (Figure 5D and 5F). BMP2 treatment enhanced the rate of scratch closure, an action that was blocked by treatment with recombinant gremlin 1 (Figure 5D and 5F). Hypoxia-conditioned medium blocked the BMP2-induced scratch closure in a manner similar to recombinant gremlin 1 (Figure 5E and 5F). Addition of the anti-gremlin antibody to hypoxia-conditioned medium from endothelial cells abolished the inhibitory action of the medium on BMP2-induced scratch closure (Figure 5E and 5F). These data show that hypoxia stimulates gremlin secretion from human pulmonary microvascular endothelial cells and that this secreted gremlin can block both BMP signaling in the endothelium and BMP-induced regeneration and repair.

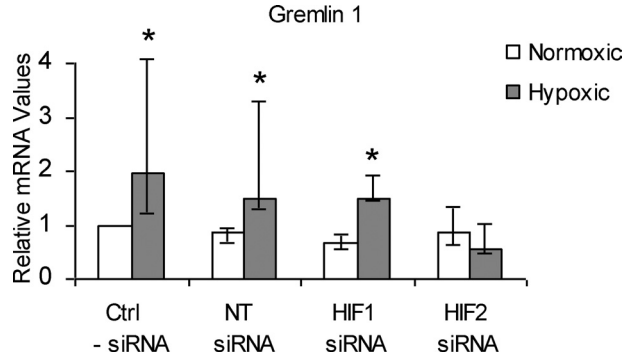

Figure 3. Hypoxia-induced increases in gremlin 1 expression in pulmonary endothelial cells required hypoxia-inducible factor (HIF)-2α. Under control conditions in the absence of siRNA (ctrl-siRNA) and in the presence of nontargeting siRNA (NT siRNA), hypoxia (48-hour exposure) caused significant increases in gremlin 1 expression (median±interquartile range). siRNA-mediated knockdown of HIF1α did not alter the hypoxia-induced increase in gremlin expression (HIF1α siRNA). However, siRNA-mediated knockdown of HIF2α completely blocked the hypoxic response of gremlin (HIF2α siRNA). Note that under normoxic conditions none of the 3 siRNAs significantly altered gremlin expression (nontargeting, siRNA targeting HIF1α, and siRNA targeting HIF2α). *$P<0.05$, significantly different from matched normoxic group.

Haplodeficiency of Gremlin 1 Attenuates Hypoxia-Induced Increases in Pulmonary Vascular Resistance

To test the hypothesis that gremlin 1 contributes significantly to the development of pulmonary hypertension in vivo, we examined changes in pulmonary vascular resistance in response to sustained hypoxia in mice with haplodeficiency of gremlin 1 caused by monozygous null mutations ($grem1^{+/-}$); homozygous loss of gremlin 1 ($grem1^{-/-}$) causes embryonic or perinatal lethality.[20] Haplodeficient mice showed reduced expression of gremlin 1 and enhanced BMP signaling in both normoxia and hypoxia (Figure XA and XB in the online-only Data Supplement). The effect of haplodeficiency of gremlin 1 on the development of pulmonary hypertension was tested by exposing wild-type and $grem1^{+/-}$ mice to hypoxia (FIO_2= 0.10) for 3 weeks. Pulmonary vascular resistance in the $grem1^{+/-}$ mice was significantly less than that in the wild-type group (Figure 6A) after hypoxic exposure. Hypoxic

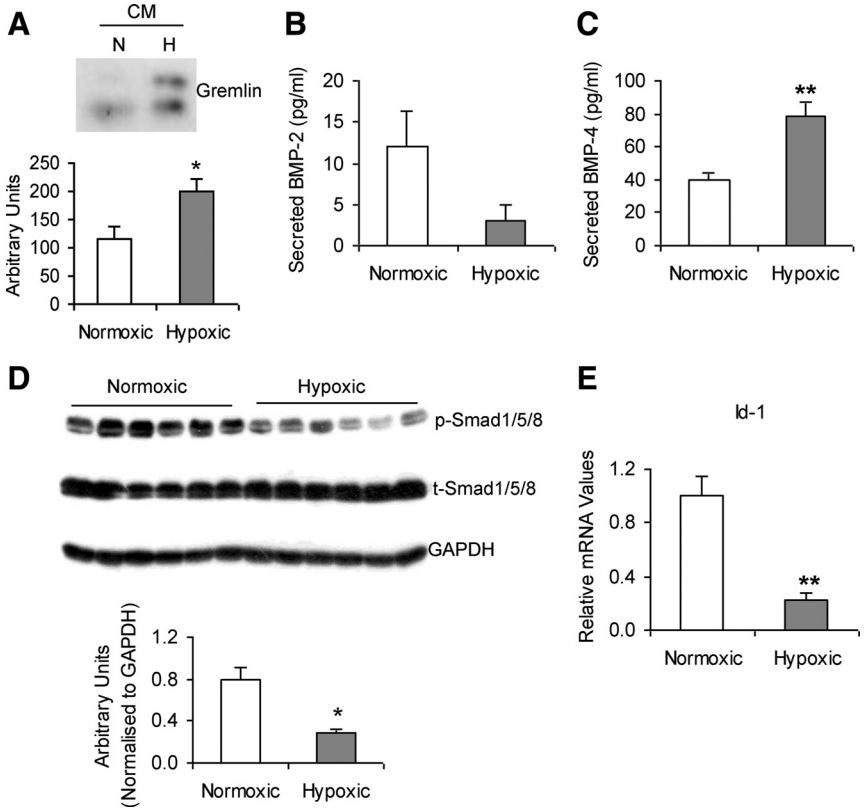

Figure 4. Endogenous gremlin 1 expression and bone morphometric protein (BMP) 2, BMP4, and BMP signaling are altered in human pulmonary microvascular endothelial cells in response to hypoxia (2 days). **A**, Western blot demonstrating increased gremlin 1 concentration in cell culture medium (CM) after hypoxic exposure (mean±SE; n=6). **B**, BMP2 concentration (mean±SE) in cell culture medium was not significantly altered ($P=0.07$) with hypoxia (n=6), whereas (**C**) BMP4 concentration (mean±SE) was enhanced (n=6). **D**, Western blot showing that Smad1/5/8 phosphorylation (mean±SE) was reduced in hypoxia (n=6). **E**, *Id1* mRNA expression (mean±SE) was downregulated after hypoxic exposure (n=6). Cells were exposed to hypoxia for 48 hours in all experiments (n=6). *$P<0.05$ and **$P<0.01$, significantly different from matched normoxic group.

pulmonary vascular resistance in wild-type mice increased by 85±3.2% of the mean normoxic value, whereas that in the haplodeficient group increased by significantly ($P<0.01$) less (63±4.3%). Thus, gremlin 1 haplodeficiency attenuated the hypoxia-induced increase in pulmonary vascular resistance. The ratio of right ventricular to left ventricular plus septal weight was significantly increased in both hypoxic grem1$^{+/-}$ and wild-type mice compared with the matched normoxic groups (Figure 6B).

In contrast to the reduced pulmonary vascular resistance observed in hypoxia, grem1$^{+/-}$ mice showed an elevation of hematocrit similar to that in wild-type mice (Figure 6C), demonstrating that the extrapulmonary, HIF-mediated erythropoietic response was unaffected by gremlin 1 haplodeficiency.[28]

Haplodeficiency of Gremlin 1 Attenuates Hypoxic Pulmonary Vascular Remodeling

The increased pulmonary vascular resistance caused by chronic hypoxia has 2 components: vasoconstriction and structural reduction in lumen diameter caused by vascular remodeling. To assess the vasoconstrictor element, we used the potent rho kinase inhibitor and vasodilator Y27632.[2] We observed small reductions in resistance in normoxic lungs (Figure 6D) as expected. In chronically hypoxic lungs, rho kinase inhibition caused significant reductions in resistance (≈40% of the chronic hypoxia-induced increase) that were similar in wild-type and grem1$^{+/-}$ mice (Figure 6D). However, in both wild-type and grem1$^{+/-}$ mouse lungs, pulmonary vascular resistance remained significantly above the normoxic value after rho kinase inhibition (Table II in the online-only Data Supplement). These data demonstrated that haplodeficiency of gremlin 1 did not alter chronic hypoxia-induced vasoconstriction.

After sustained hypoxic exposure, the walls of small intra-acinar vessels of wild-type mice showed characteristic thickening in response to 3 weeks of hypoxia, which was reduced in the hypoxic grem1$^{+/-}$ mice (Figure 7A). Wild-type mice showed a typical increase in lung volume in response to sustained hypoxia, which was not observed in grem1$^{+/-}$ mice (Figure XI in the online-only Data Supplement). Stereological analysis showed that wall thickness in the smaller intra-acinar vessels of hypoxic lungs was significantly less in grem1$^{+/-}$ mice than in wild-type mice (Figure 7B). In wild-type mice, sustained hypoxia caused a significant reduction in mean lumen diameter of these vessels, which was not observed in grem1$^{+/-}$ mice (Figure 7C). The mean total length of intra-acinar vessels was unchanged by chronic hypoxia in both wild-type and grem1$^{+/-}$ mice (Figure 7D), although interestingly length density was reduced in hypoxic lungs (Table I in the online-only Data Supplement). The volume and length of vessels in the smallest-diameter category were significantly increased in the grem1$^{+/-}$ mice after hypoxic exposure, although to a lesser extent than in wild-type mice (Figure 7E and 7F). These data show that in wild-type mice there was a reduction in the lumen diameter of the intra-acinar vessels, leading to an increase in the length of vessels included in the smallest category (10–20 μm). Because of the inverse fourth-power relationship between radius and vascular resistance (the Poiseuille equation), the reduction in mean lumen diameter (≈10%) in wild-type mice (Figure 7C) could completely account for the structural component of the increased vascular resistance (Table II in

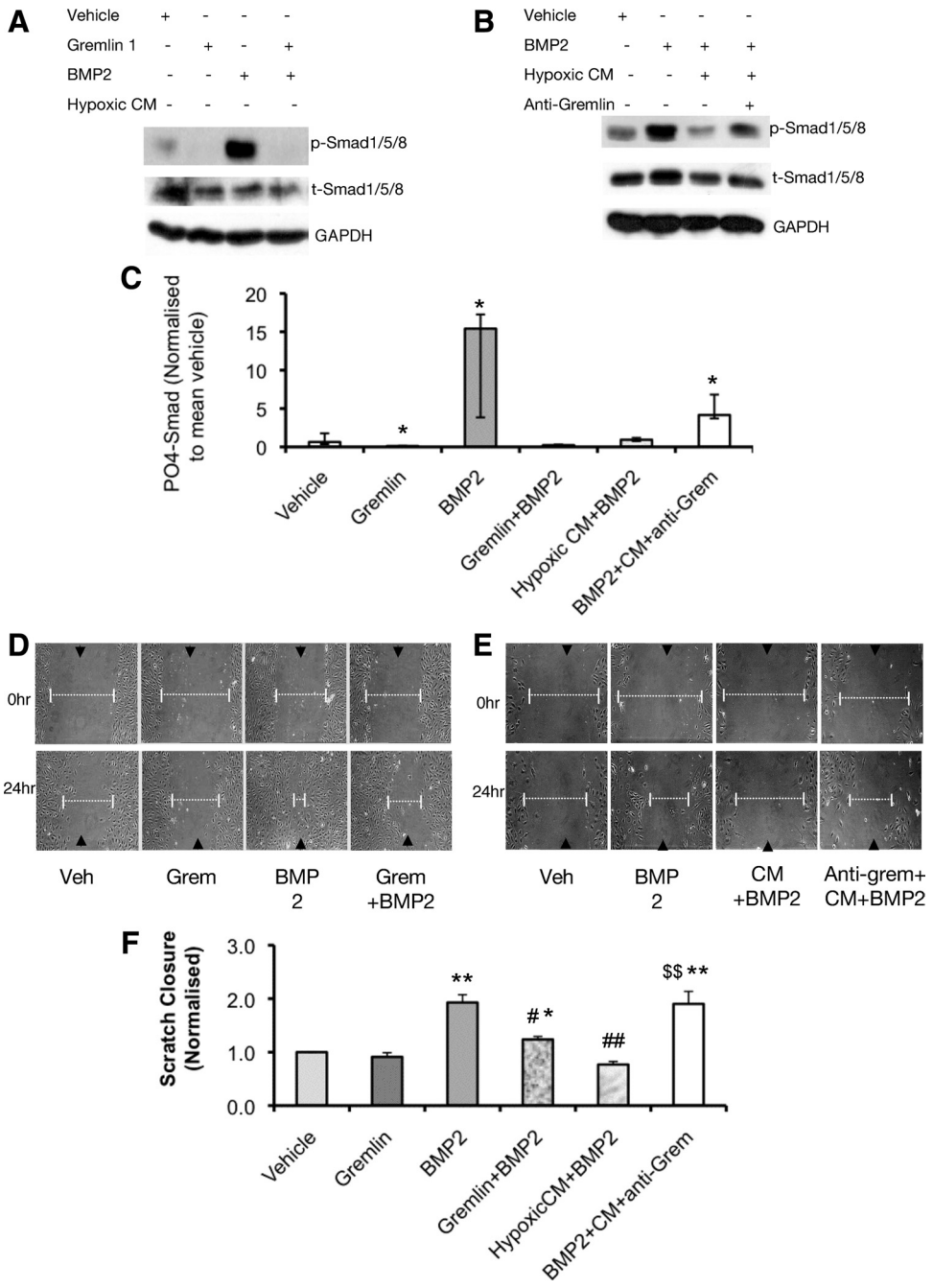

Figure 5. Hypoxia-induced gremlin 1 secretion blocks bone morphometric protein (BMP) signaling and scratch closure in pulmonary microvascular endothelial cells. **A**, Exogenous BMP2 (100 ng/mL) induced Smad1/5/8 phosphorylation, which was blocked by exogenous gremlin 1 (2 μg/mL). **B**, Hypoxia-conditioned medium blocked BMP2 (100 ng/mL)-induced Smad1/5/8 phosphorylation, which was restored by preincubating hypoxic conditioned medium (CM) with anti-gremlin antibody (15 μg/mL). **C**, Densitometric (median±interquartile range) analysis of phospho (p)-Smad blots. Vehicle (n=9), gremlin (n=6), BMP (n=9), gremlin+BMP2 (n=6), hypoxic CM+BMP2 (n=6), BMP2+CM+anti-gremlin antibodies (n=6). **D**, BMP2 (100 ng/mL) induced scratch closure (measured at 24 hours), which was blocked by recombinant gremlin 1 (2 μg/mL) and restored by preincubating hypoxic CM with anti-gremlin antibody (15 μg/mL). **E**, BMP2 (100 ng/mL) treatment–induced scratch closure was blocked by hypoxic CM in a manner similar to blockade by recombinant gremlin 1 and restored by anti-gremlin antibody (15 μg/mL). **F**, Scratch healing (mean±SEM) in all groups. Vehicle (Veh; n=9), gremlin (Grem; n=6), BMP2 (n=9), gremlin+BMP2 (n=6), hypoxic CM+BMP2 (n=6), BMP2+CM+anti-gremlin antibody (n=6). *$P<0.05$ and **$P<0.01$, significantly different from vehicle-treated cells. #$P<0.05$ and ##$P<0.01$, significantly different from BMP2-treated cells. $$$P<0.01$, significantly different from hypoxic CM+BMP2-treated cells.

the online-only Data Supplement). In contrast, in the haploinsufficient mouse lungs, these structural changes were significantly attenuated, markedly reducing the structurally mediated increases in resistance (Table II in the online-only Data Supplement).

Gremlin Expression in Vessels of Explanted Human PAH Lungs

Immunohistochemical staining of sections taken from lungs explanted from patients with IPAH and HPAH showed staining for gremlin that suggested endothelial localization

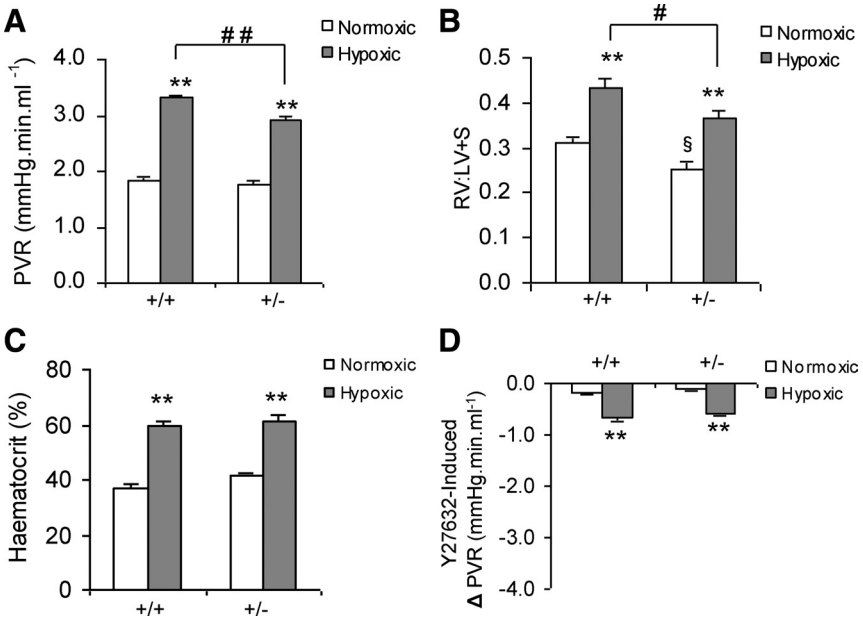

Figure 6. Hypoxia-induced increase in pulmonary vascular resistance (PVR) is reduced in grem1$^{+/-}$ mice. **A**, PVR (mean±SE) is reduced in hypoxic grem1$^{+/-}$ compared with hypoxic wild-type mice (n=17–20). **B**, The ratio (mean±SE) of right ventricular to left ventricular+septum weights (RV:LV+S) in response to sustained hypoxic exposure was significantly less in the grem1$^{+/-}$ mice compared with the wild-type group (n=9–10 per group). **C**, Hematocrit levels (mean±SE) were significantly increased to similar values in response to 3 weeks of hypoxic exposure in both wild-type and grem1$^{+/-}$ mice (n=9–10). **D**, The reduction in PVR induced by Rho kinase inhibition (Y27632; 10^{-5} mol/L; mean±SE) was similar in hypoxic wild-type and hypoxic grem1$^{+/-}$ mouse lungs (n=8). #$P<0.05$ and ##<0.01, significantly different from hypoxic wild-type groups. **$P<0.01$, significantly different from matched normoxic groups.

(Figure 8A–8D), which was more marked than that observed in control lungs (Figure 8E–H). Gremlin was not seen in the cells of the immediately adjacent vascular wall, either in the remodeled vessels in PAH or in normal lungs, suggesting that the endothelium was the predominant source of gremlin in the small resistance vessel walls. In plexiform lesions, immunostaining was variable, with some vascular channels demonstrating intense staining and others showing much less or absent staining (Figure 8I–8N).

Discussion

We report here that the BMP antagonist gremlin was increased in the walls of the small vessels of the pulmonary circulation in vivo during the development of hypoxic pulmonary hypertension. Hypoxia increased gremlin secretion from endothelial cells in vitro, which blocked BMP signaling in and regeneration of endothelial cell monolayers. Haplodeficiency of gremlin 1 prevented the reduction of BMP signaling observed in wild-type hypoxic mouse lung in vivo, inhibited pulmonary vascular remodeling, and thus attenuated the development of increased pulmonary vascular resistance without altering hypoxic vasoconstriction. Furthermore, gremlin was increased in the small pulmonary vessels of the explanted lungs from patients with HPAH and IPAH.

Gremlin 1 was originally identified as a gene that encodes a small glycoprotein (23–28 kDa) that binds noncovalently to specific ligands of the BMP family (BMP2, BMP4, and BMP7), thus preventing interaction with BMPR1 and BMPR2.[6] After glycosylation and secretion, gremlin 1 binds noncovalently to the cell surface and extracellular matrix, thus tending to act locally to reduce the effective free concentration of BMPs and to inhibit signaling in cells closely adjacent to its sites of production.[29] Gremlin 1 is highly expressed in the mouse lung during embryonic development[6]; moreover, homozygous deletion of gremlin 1 prevents normal lung development as a result of reduced septation.[20] Overexpression of gremlin 1 in the lung during development also impairs normal lung formation by disrupting normal airway branching and formation.[6] Thus, the balanced actions of BMPs and gremlin 1, coordinated both spatially and temporally, are required for normal lung development.

Attenuation of BMP signaling specifically in the endothelium by selective deletion of BMPR2 is sufficient to cause pulmonary vascular remodeling and the spontaneous development of pulmonary hypertension in mice.[11] In keeping with this, the endothelium is the predominant site of BMPR2 expression in the normal pulmonary vessels, and normal BMP signaling is required for survival of pulmonary endothelial cells.[11,14,30,31] Conversely, overexpression of BMPR2 in the endothelium protected mice against the development of hypoxic pulmonary hypertension.[32] BMPR signaling in pulmonary vascular smooth muscle cells is also required to maintain low vascular smooth muscle tone, to prevent abnormal proliferation, and to maintain normal medial structure.[10,33] Recent evidence demonstrates that BMP2 produced by the endothelium is the major BMP ligand activating the BMPRs in the pulmonary vascular wall.[7] These data show that endothelial BMP signaling is essential for homeostatic maintenance of normal pulmonary vascular structure and function. Thus, the increased gremlin expression and secretion from the hypoxic pulmonary endothelium that we have demonstrated are optimally placed to inhibit the actions of BMP2 secreted by the pulmonary endothelium, which are required to maintain normal pulmonary vascular resistance.[7] Increased gremlin may not be the only reason for reduced BMP mediated signaling; we also demonstrated reduced BMP2 and BMPR2 expression in the hypoxic lung (Figure 2). Nonetheless, our finding that mono-allelic loss of gremlin was sufficient to attenuate the hypoxia-induced increase in pulmonary vascular resistance emphasizes the importance of this molecule in the pathogenesis of the disease. These results underestimate the effects of gremlin because, in the haplodeficient mouse, gremlin expression, although reduced, was still

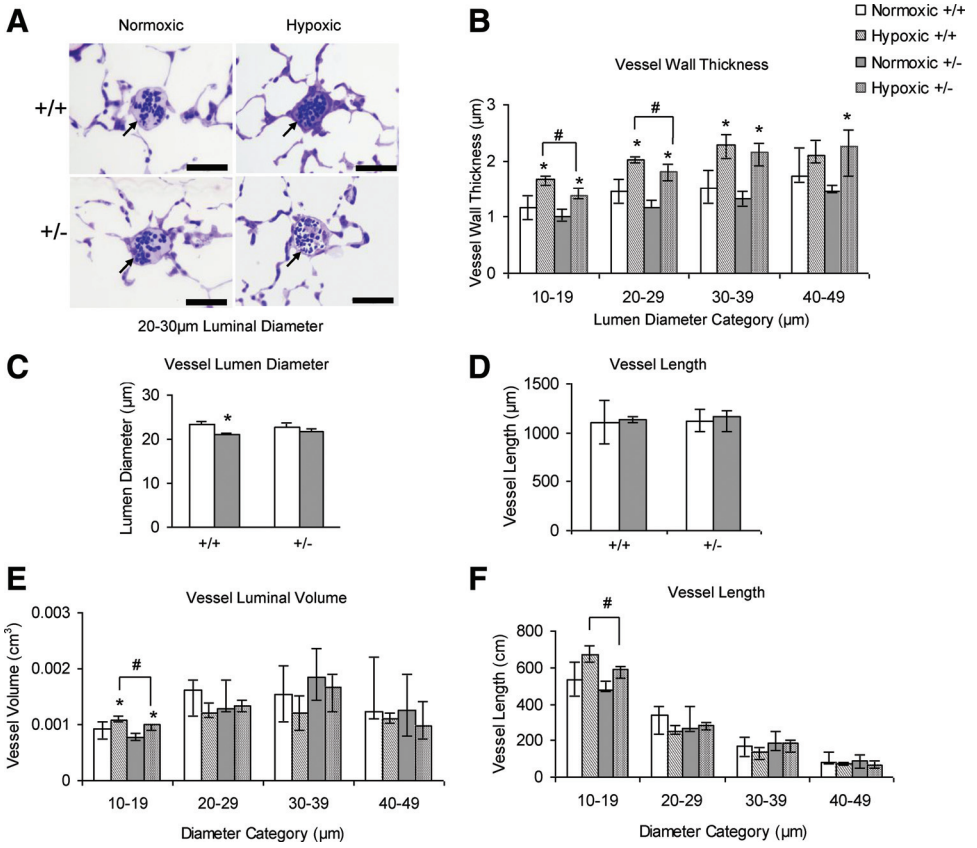

Figure 7. Grem1$^{+/-}$ mice show reduced pulmonary vascular remodeling. **A**, Representative images of small intra-acinar vessels (arrows) in wild-type and grem1$^{+/-}$ mice (×40 objective; scale bars=50 μm). **B**, Vessel wall thickness (median±interquartile range) within each vessel size category (based on lumen diameter) was significantly less in the smaller vessels in grem1$^{+/-}$ mice compared with wild-type mice after 3 weeks of hypoxic exposure (n=8 per group). **C**, The mean lumen diameter (mean±SE) was significantly decreased in wild-type mice after 3 weeks of hypoxic exposure but was not significantly altered in grem1$^{+/-}$ mice. **D**, The total length of intra-acinar vessels (median±interquartile range) was similar in both normoxic and hypoxic wild-type and grem1$^{+/-}$ groups. **E**, The volume of the vessel lumen (median±interquartile range) within each size category of vessel in normoxic and hypoxic condition in wild-type and grem1$^{+/-}$ mouse lungs and (**F**) the length of vessel (median±interquartile range) within each vessel category. Within the smallest category, volume and length were increased after sustained hypoxia, although these changes were significantly less in the grem1$^{+/-}$ group. #$P<0.05$, significantly different from hypoxic wild-type group. *$P<0.05$, significantly different from matched normoxic group of same genotype.

present and increased in response to hypoxia, although to lower levels and with less effect on BMP signaling than in hypoxic wild-type mice. Taken together, these data provide evidence for a novel autocrine-paracrine axis consisting of the balanced actions of BMP2, BMP4, and gremlin 1 operating homeostatically in the pulmonary vascular endothelium and adjacent vessel wall to maintain the normal pulmonary vascular structure and function.

Our data suggest that alveolar hypoxia such as that found in lung diseases stimulates the pulmonary microvascular endothelium to secrete gremlin 1. Given that haplodeficiency of HIF2α in mice prevents the development of hypoxic pulmonary hypertension,[34] it is interesting that the hypoxia-induced increases in gremlin 1 expression in pulmonary microvascular endothelial cells required HIF2α. Moreover, pulmonary hypertension in the HIF2α-deficient mouse was prevented by reduced pulmonary vascular remodeling without any effect on acute hypoxic vasoconstriction, a pattern of change similar to that which we observed in grem1$^{+/-}$ mice.[34] Although we provide evidence that HIF2α is required for hypoxic induction of gremlin 1 expression in the pulmonary microvascular endothelium, it remains to be determined how it acts in this context. HIF controls gene expression directly by binding to hypoxia response elements in the proximal promoter but also at sites remote from the regulated gene.[26,35] HIF also regulates genes indirectly by interactions with other transcription factors, by stabilization of mRNAs, and by regulation of microRNAs.[35–40] Taken together, these data provide an explanation for the reduction in BMP signaling previously reported in chronically hypoxic hypertensive lungs in the absence of BMPR2 mutations.[15] Furthermore, because the hypoxic increase in gremlin 1 is restricted to the lung and is not observed in other organs, these data identify a mechanism that can account for the structural component of the increase in vascular resistance in response to sustained hypoxia, which is unique to the pulmonary circulation, such as that observed in chronic lung diseases and at high altitude.[17]

Pulmonary vascular remodeling occurs rapidly after the onset of alveolar hypoxia (within the first day) and is largely completed within a few weeks. In their classic studies, Meyrick and Reid[41] showed that cellular proliferation in the

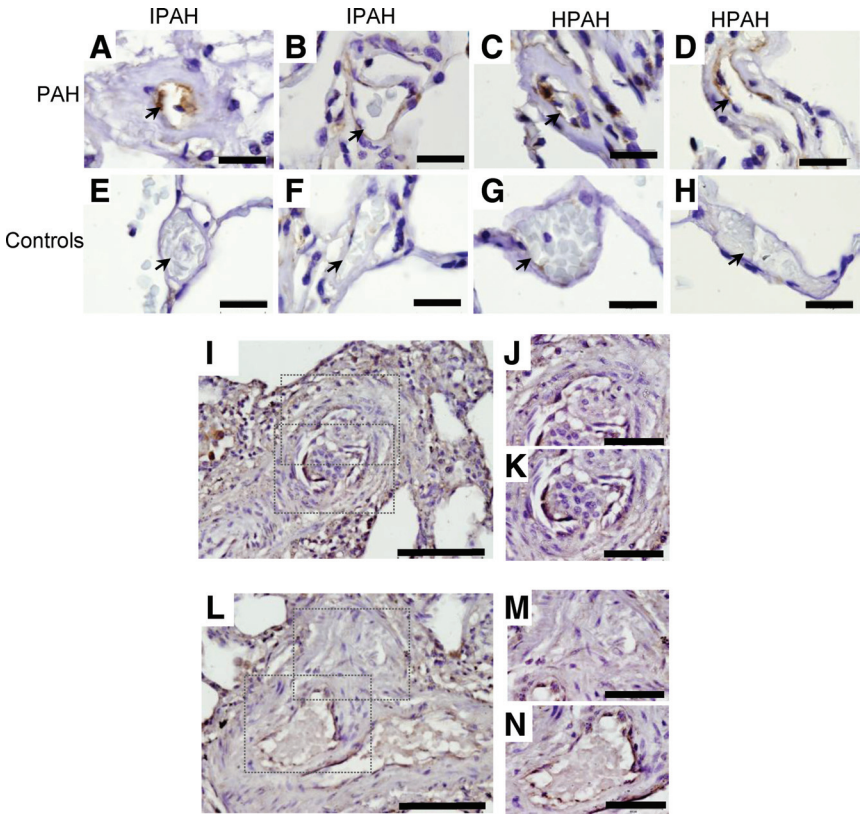

Figure 8. Gremlin expression in the pulmonary vascular endothelium of lungs explanted from subjects with pulmonary arterial hypertension (PAH). Representative images of sections from 2 idiopathic PAH (IPAH; **A** and **B**), 2 rare heritable form of PAH (HPAH; **C** and **D**), and 4 control (**E–H**) lungs showing gremlin immunohistochemical staining (brown; arrowheads). Low-intensity staining was observed in vessels in control lungs; there was marked staining in the small remodeled vessels in the hypertensive lungs in a pattern compatible with endothelial localization (×100 objective; scale bar=20 μm). In plexiform lesions (**I** and **L**), endothelial immunostaining was variable (×40 objective; scale bar=100 μm), with some vascular channels demonstrating intense staining (**J, K,** and **N**) and others showing no staining (**M**; ×100 objective; scale bar=50 μm).

pulmonary vasculature of hypoxic rats peaked during the first week and then declined to baseline after 14 days; medial and adventitial hypertrophy reached a plateau after 10 days and then remained stable during continued exposure. Thus, blocking active remodeling during this early period could have sustained effects on pulmonary vascular structure. It is interesting that this corresponds to the period during which gremlin rises to its peak expression and returns to baseline in hypoxic wild-type mice (Figure 1). Our results in haploinsufficient mice show that a reduction in gremlin 1 during that early period attenuates the hypoxia-induced increase in pulmonary vascular resistance. However, we also found changes in other elements of the BMP signaling pathway, including both BMP ligands and BMPR (Figures 2 and 4). Furthermore, gremlin can act by mechanisms that are independent of its extracellular blockade of BMP ligands, including the vascular endothelial growth factor pathway, Slit-Robo interactions, and intracellular mechanisms.[6,42] Thus, the longer-term effects (>3 weeks of hypoxia) of gremlin haploinsufficiency on both signaling and vascular resistance in pulmonary hypertension remain to be elucidated.

In idiopathic pulmonary fibrosis, which causes alveolar hypoxia and vascular loss, pulmonary hypertension is a prominent feature and is associated with a poor prognosis.[43] Recently, it has been reported that gremlin 1 expression is significantly increased in idiopathic pulmonary fibrosis lungs, which, in the light of our results, suggests that gremlin 1 may play an important role in causing pulmonary hypertension in this disease.[44] Because the hypoxia-induced increase in gremlin 1 is selective for the lung, it offers an attractive potential target for therapy because antagonism of its actions might have minimal effects in other organs.

Our finding of increased gremlin expression in the walls of pulmonary vessels in explanted lungs from patients with IPAH and HPAH in a pattern compatible with endothelial expression suggests that gremlin may play a pathogenic role in these and other forms of PAH not caused by alveolar hypoxia. Furthermore, the high basal levels of both gremlin 1 and gremlin 2 in the lung may render it particularly susceptible to any further reductions in BMP signaling resulting from heterozygous mutations in BMPR2, whereas in other organs the remaining BMPR2 signaling, although haplodeficient, could be sufficient to maintain vascular homeostasis.[5]

Conclusions

We report a lung-selective, early-onset, hypoxia-induced increase in gremlin 1 expression that plays an important pathogenic role in the development of pulmonary hypertension by promoting vascular remodeling and thus increasing pulmonary vascular resistance while leaving hypoxic vasoconstriction unchanged. This finding identifies, for the first time, a molecular mechanism that accounts for the unique vascular remodeling of the pulmonary circulation in response to hypoxia. Furthermore, the high levels of expression of gremlin 1 and gremlin 2 in the lung may render it particularly vulnerable to further reductions in BMP signaling resulting from heterozygous loss-of-function mutations of BMPR2 in HPAH and thus may account for the development of vascular remodeling, increased vascular resistance, and hypertension in the pulmonary circulation while other vascular beds remain unharmed.

Sources of Funding

This study was supported by funding from the Health Research Board Ireland, HEA PRTLI, Science Foundation Ireland, and Cambridge University Hospital's National Institute of Health Research Biomedical Research Centre. Dr Cahill was supported by a University College Dublin Ad Astra Research Scholarship. S. Harkin was supported by an Association of Physicians of Great Britain and Ireland Scholarship. Dr Morrell is supported by the British Heart Foundation.

Disclosures

None.

References

1. Rabinovitch M. Molecular pathogenesis of pulmonary arterial hypertension. *J Clin Invest*. 2008;118:2372–2379.
2. Hyvelin J-M, Howell K, Nichol A, Costello CM, Preston RJ, McLoughlin P. Inhibition of rho-kinase attenuates hypoxia-induced angiogenesis in the pulmonary circulation. *Circ Res*. 2005;97:185–191.
3. Naeije R. Pulmonary hypertension and right heart failure in chronic obstructive pulmonary disease. *Proc Am Thorac Soc*. 2005;2:20–22.
4. Humbert M, Sitbon O, Chaouat A, Bertocchi M, Habib G, Gressin V, Yaici A, Weitzenblum E, Cordier JF, Chabot F, Dromer C, Pison C, Reynaud-Gaubert M, Haloun A, Laurent M, Hachulla E, Cottin V, Degano B, Jais X, Montani D, Souza R, Simonneau G. Survival in patients with idiopathic, familial, and anorexigen-associated pulmonary arterial hypertension in the modern management era. *Circulation*. 2010; 122:156–163.
5. Machado RD, Pauciulo MW, Thomson JR, Lane KB, Morgan NV, Wheeler L, Phillips JA 3rd, Newman J, Williams D, Galiè N, Manes A, McNeil K, Yacoub M, Mikhail G, Rogers P, Corris P, Humbert M, Donnai D, Martensson G, Tranebjaerg L, Loyd JE, Trembath RC, Nichols WC. BMPR2 haploinsufficiency as the inherited molecular mechanism for primary pulmonary hypertension. *Am J Hum Genet*. 2001;68:92–102.
6. Costello CM, Cahill E, Martin F, Gaine S, McLoughlin P. Role of gremlin in the lung: development and disease. *Am J Respir Cell Mol Biol*. 2010;42:517–523.
7. Anderson L, Lowery JW, Frank DB, Novitskaya T, Jones M, Mortlock DP, Chandler RL, de Caestecker MP. Bmp2 and Bmp4 exert opposing effects in hypoxic pulmonary hypertension. *Am J Physiol Regul Integr Comp Physiol*. 2009;298:R833–R842.
8. Frank DB, Abtahi A, Yamaguchi DJ, Manning S, Shyr Y, Pozzi A, Baldwin HS, Johnson JE, de Caestecker MP. Bone morphogenetic protein 4 promotes pulmonary vascular remodeling in hypoxic pulmonary hypertension. *Circ Res*. 2005;97:496–504.
9. Morty RE, Nejman B, Kwapiszewska G, Hecker M, Zakrzewicz A, Kouri FM, Peters DM, Dumitrascu R, Seeger W, Knaus P, Schermuly RT, Eickelberg O. Dysregulated bone morphogenetic protein signaling in monocrotaline-induced pulmonary arterial hypertension. *Arterioscler Thromb Vasc Biol*. 2007;27:1072–1078.
10. Song Y, Jones JE, Beppu H, Keaney JF Jr, Loscalzo J, Zhang Y-Y. Increased susceptibility to pulmonary hypertension in heterozygous BMPR2-mutant mice. *Circulation.* 2005;112:553–562.
11. Hong K-H, Lee YJ, Lee E, Park SO, Han C, Beppu H, Li E, Raizada MK, Bloch KD, Oh SP. Genetic ablation of the BMPR2 gene in pulmonary endothelium is sufficient to predispose to pulmonary arterial hypertension. *Circulation*. 2008;118:722–730.
12. Yanagita M. BMP antagonists: their roles in development and involvement in pathophysiology. *Cytokine Growth Factor Rev*. 2005;16: 309–317.
13. Derynck R, Zhang YE. Smad-dependent and Smad-independent pathways in TGF-[beta] family signalling. *Nature*. 2003;425:577–584.
14. Takahashi K, Kogaki S, Matsushita T, Nasuno S, Kurotobi S, Ozono K. Hypoxia induces alteration of bone morphogenetic protein receptor signaling in pulmonary artery endothelial cell. *Pediatr Res.* 2007;61: 392–397.
15. Long L, Crosby A, Yang X, Southwood M, Upton PD, Kim D-K, Morrell NW. Altered bone morphogenetic protein and transforming growth factor-{beta} signaling in rat models of pulmonary hypertension: potential for activin receptor-like kinase-5 inhibition in prevention and progression of disease. *Circulation*. 2009;119:566–576.
16. Newman JH, Phillips JA, Loyd JE. Narrative review: the enigma of pulmonary arterial hypertension: new insights from genetic studies. *Ann Intern Med*. 2008;148:278–283.
17. Costello CM, Howell K, Cahill E, McBryan J, Konigshoff M, Eickelberg O, Gaine S, Martin F, McLoughlin P. Lung-selective gene responses to alveolar hypoxia: potential role for the bone morphogenetic antagonist gremlin in pulmonary hypertension. *Am J Physiol Lung Cell Mol Physiol*. 2008;295:L272–284.
18. Walsh DW, Godson C, Brazil DP, Martin F. Extracellular BMP-antagonist regulation in development and disease: tied up in knots. *Trends Cell Biol*. 2010;20:244–256.
19. Roxburgh SA, Kattla JJ, Curran SP, O'Meara YM, Pollock CA, Goldschmeding R, Godson C, Martin F, Brazil DP. Allelic depletion of grem1 attenuates diabetic kidney disease. *Diabetes*. 2009;58:1641–1650.
20. Michos O, Panman L, Vintersten K, Beier K, Zeller R, Zuniga A. Gremlin-mediated BMP antagonism induces the epithelial-mesenchymal feedback signaling controlling metanephric kidney and limb organogenesis. *Development*. 2004;131:3401–3410.
21. Howell K, Costello CM, Sands M, Dooley I, McLoughlin P. L-Arginine promotes angiogenesis in the chronically hypoxic lung: a novel mechanism ameliorating pulmonary hypertension. *Am J Physiol Lung Cell Mol Physiol*. 2009;296:L1042–L1050.
22. Cadogan E, Hopkins N, Giles S, Bannigan JG, Moynihan J, McLoughlin P. Enhanced expression of inducible nitric oxide synthase without vasodilator effect in chronically infected lungs. *Am J Physiol Lung Cell Mol Physiol*. 1999;277:L616–L627.
23. Ludbrook J. Multiple comparison procedures updated. *Clin Exp Pharmacol Physiol*. 1998;25:1032–1037.
24. Meyrick B, Reid L. Ultrastructural features of the distended pulmonary arteries of the normal rat. *Anat Rec*. 1979;193:71–97.
25. Chan MC, Weisman AS, Kang H, Nguyen PH, Hickman T, Mecker SV, Hill NS, Lagna G, Hata A. The amiloride derivative phenamil attenuates pulmonary vascular remodeling by activating NFAT and the bone morphogenetic protein signaling pathway. *Mol Cell Biol.* 31:517–530.
26. Schodel J, Oikonomopoulos S, Ragoussis J, Pugh CW, Ratcliffe PJ, Mole DR. High-resolution genome-wide mapping of HIF-binding sites by ChIP-seq. *Blood*. 2011;117:e207–e217.
27. Elvidge GP, Glenny L, Appelhoff RJ, Ratcliffe PJ, Ragoussis J, Gleadle JM. Concordant regulation of gene expression by hypoxia and 2-oxoglutarate-dependent dioxygenase inhibition: the role of HIF-1alpha, HIF-2alpha, and other pathways. *J Biol Chem*. 2006;281:15215–15226.
28. Semenza GL. Involvement of oxygen-sensing pathways in physiologic and pathologic erythropoiesis. *Blood*. 2009;114:2015–2019.
29. Topol LZ, Bardot B, Zhang Q, Resau J, Huillard E, Marx M, Calothy G, Blair DG. Biosynthesis, post-translation modification, and functional characterization of DRM/gremlin. *J Biol Chem*. 2000;275:8785–8793.
30. Atkinson C, Stewart S, Upton PD, Machado R, Thomson JR, Trembath RC, Morrell NW. Primary pulmonary hypertension is associated with reduced pulmonary vascular expression of type II bone morphogenetic protein receptor. *Circulation*. 2002;105:1672–1678.
31. Teichert-Kuliszewska K, Kutryk MJB, Kuliszewski MA, Karoubi G, Courtman DW, Zucco L, Granton J, Stewart DJ. Bone morphogenetic protein receptor-2 signaling promotes pulmonary arterial endothelial cell survival: implications for loss-of-function mutations in the pathogenesis of pulmonary hypertension. *Circ Res*. 2006;98:209–217.
32. Reynolds A, Xia W, Holmes M, Hodge S, Danilov S, Curiel D, Morrell N, Reynolds P. Bone morphogenetic protein type 2 receptor gene therapy attenuates hypoxic pulmonary hypertension. *Am J Physiol Lung Cell Mol Physiol*. 2007;292:L1182–L1192.
33. West J, Harral J, Lane K, Deng Y, Ickes B, Crona D, Albu S, Stewart D, Fagan K. Mice expressing bmpr2r899x transgene in smooth muscle develop pulmonary vascular lesions. *Am J Physiol Lung Cell Mol Physiol*. 2008;295:L744–L755.
34. Brusselmans K, Compernolle V, Tjwa M, Wiesener MS, Maxwell PH, Collen D, Carmeliet P. Heterozygous deficiency of hypoxia-inducible factor-2alpha protects mice against pulmonary hypertension and right ventricular dysfunction during prolonged hypoxia. *J Clin Invest*. 2003; 111:1519–1527.
35. Mole DR, Blancher C, Copley RR, Pollard PJ, Gleadle JM, Ragoussis J, Ratcliffe PJ. Genome-wide association of hypoxia-inducible factor (HIF)-1alpha and HIF-2alpha DNA binding with expression profiling of hypoxia-inducible transcripts. *J Biol Chem*. 2009;284:16767–16775.
36. Chu SH, Feng DF, Ma YB, Zhu ZA, Zhang H, Qiu JH. Stabilization of hepatocyte growth factor mRNA by hypoxia-inducible factor 1. *Mol Biol Rep*. 2009;36:1967–1975.

37. Koshiji M, Kageyama Y, Pete EA, Horikawa I, Barrett JC, Huang LE. Hif-1alpha induces cell cycle arrest by functionally counteracting myc. *EMBO J*. 2004;23:1949–1956.
38. Pantuck AJ, An J, Liu H, Rettig MB. NF-kappab-dependent plasticity of the epithelial to mesenchymal transition induced by von Hippel-Lindau inactivation in renal cell carcinomas. *Cancer Res*. 2010;70:752–761.
39. Bermudez O, Jouandin P, Rottier J, Bourcier C, Pages G, Gimond C. Post-transcriptional regulation of the DUSP6/MKP-3 phosphatase by MEK/ERK signaling and hypoxia. *J Cell Physiol*. 2011;226:276–284.
40. Ikeda E, Achen MG, Breier G, Risau W. Hypoxia-induced transcriptional activation and increased mRNA stability of vascular endothelial growth factor in C6 glioma cells. *J Biol Chem*. 1995;270:19761–19766.
41. Meyrick B, Reid L. Hypoxia and incorporation of 3H-thymidine by cells of the rat pulmonary arteries and alveolar wall. *Am J Pathol*. 1979;96:51–70.
42. Mitola S, Ravelli C, Moroni E, Salvi V, Leali D, Ballmer-Hofer K, Zammataro L, Presta M. Gremlin is a novel agonist of the major proangiogenic receptor VEGFR2. *Blood*. 2011;116:3677–3680.
43. Nathan SD, Noble PW, Tuder RM. Idiopathic pulmonary fibrosis and pulmonary hypertension: connecting the dots. *Am J Respir Crit Care Med*. 2007;175:875–880.
44. Myllarniemi M, Lindholm P, Ryynanen MJ, Kliment CR, Salmenkivi K, Keski-Oja J, Kinnula VL, Oury TD, Koli K. Gremlin-mediated decrease in bone morphogenetic protein signaling promotes pulmonary fibrosis. *Am J Respir Crit Care Med*. 2008;177:321–329.

CLINICAL PERSPECTIVE

Pulmonary hypertension is a disease characterized by pulmonary vascular remodeling and increased pulmonary vascular resistance. It occurs commonly in chronic hypoxic lung diseases and leads to increased morbidity and mortality. A major breakthrough in our understanding of pulmonary hypertension was achieved with the identification of heterozygous mutations in the bone morphogenetic receptor type 2 as the cause of the rare heritable form of pulmonary arterial hypertension. It was subsequently found that bone morphogenetic protein signaling was reduced in many other common forms of pulmonary hypertension, including hypoxic pulmonary hypertension. However, the mechanism underlying this reduction has not been clearly elucidated. Here, we report that gremlin, a secreted extracellular antagonist of bone morphogenetic proteins, was expressed more highly in pulmonary endothelial cells in vitro than in the endothelium of other organs and was markedly increased in response to hypoxia. We show that gremlin was increased selectively in the hypoxic mouse lung and that genetically manipulated mice with reduced gremlin expression showed attenuation of hypoxic pulmonary vascular remodeling and reduced pulmonary vascular resistance. Furthermore, we found that gremlin was increased in the small intrapulmonary vessels of lungs explanted from patients with pulmonary arterial hypertension. Thus, we have identified a novel mechanism contributing to the development of pulmonary hypertension, which, because it is an extracellular protein, represents an attractive potential therapeutic target.

Gremlin Plays a Key Role in the Pathogenesis of Pulmonary Hypertension

Edwina Cahill, Christine M. Costello, Simon C. Rowan, Susan Harkin, Katherine Howell, Martin O. Leonard, Mark Southwood, Eoin P. Cummins, Susan F. Fitzpatrick, Cormac T. Taylor, Nicholas W. Morrell, Finian Martin and Paul McLoughlin

Circulation. 2012;125:920-930; originally published online January 13, 2012;
doi: 10.1161/CIRCULATIONAHA.111.038125
Circulation is published by the American Heart Association, 7272 Greenville Avenue, Dallas, TX 75231

Print ISSN: 0009-7322. Online ISSN: 1524-4539

SUPPLEMENTAL MATERIAL

Gremlin plays a key role in the pathogenesis of pulmonary hypertension.

Edwina Cahill PhD[1], Christine M. Costello PhD[1], Simon C Rowan BSc[1], Susan Harkin[1], Katherine Howell PhD[1], Martin O. Leonard PhD[1], Mark Southwood PhD[3], Eoin P Cummins PhD[1], Susan F Fitzpatrick BSc[1], Cormac Taylor PhD[1], Nicholas W. Morrell MD[3], Finian Martin PhD[2], Paul McLoughlin MB BCh PhD[1,#]

[1]University College Dublin, School of Medicine and Medical Sciences and [2]School of Biomedical and Biomolecular Sciences, Dublin, Ireland and [3]University of Cambridge School of Clinical Medicine, Cambridge, United Kingdom.

[#]Correspondence should be addressed to:

Dr Paul McLoughlin MB BCh PhD.

University College Dublin,

School of Medicine and Medical Sciences,

Belfield, Dublin 4, Ireland.

e-mail. Paul.mcloughlin@ucd.ie

Phone. +353 1 716 6583. Fax. +353 1 716 6649

Supplemental Methods

Mice. All procedures involving mice were approved by the UCD Animal Research Ethics Sub-Committee and carried out under license from the Department of Health.

Chronic hypoxic pulmonary hypertension was induced by housing male C57BL/6 mice (10-12 weeks) in a hypoxic normobaric opaque perspex environmental chamber (FiO_2<0.10, $FiCO_2$<0.01) and weight-matched normoxic mice were maintained in normoxic conditions in the same room (FiO_2=0.21, $FiCO_2$<0.01). Oxygen concentrations were monitored using an automated gas analyzer (Pro-Ox and Pro-CO_2, Biospherix). The chamber was opened every 1-2 days for approximately 30 minutes to allow for changing of cages and replacement of food and water. Excess CO_2 produced by the mice was removed using a tray of soda lime placed inside the chamber. All mice were maintained in a specific pathogen-free (SPF) facility with free access to water and food.

Gremlin1 heterozygote knockout mice ($grem1^{+/-}$) were bred and pups genotyped by extracting DNA from ear punches and determining the presence of the LacZ knock-in gene by end-point PCR as described previously[1, 2].

RNA Isolation and real-time PCR. Total RNA was extracted from snap-frozen whole tissue or cells using a Qiagen RNeasy kit (RNeasy Mini Kit, Qiagen) and reverse-transcribed (RT) to cDNA using Superscript II RNase H-Reverse Transcriptase kit (Invitrogen) as previously described[3]. TaqMan real-time PCR was performed using 18S rRNA as the endogenous loading control gene. Reactions were carried out on the ABI PRISM 7900 Sequence Detection System with TaqMan Universal PCR Master Mix and TaqMan Gene Expression Assays (Applied Biosystems). Relative quantification of mRNA expression levels was determined using the standard curve method and normalised to 18S.

Immunohistochemical analysis

To obtain mouse lung sections, male C57BL/6 mice (*n*=5) were maintained in normoxia or exposed to 10% oxygen for two days. The mice were killed by exsanguination under general anesthesia, the lungs removed and then fixed by intratracheal instillation of paraformaldehyde (4%) at standard pressure (25 cm of water). The lungs were then immersed in paraformaldehyde and left overnight, cut into blocks, embedded in paraffin wax and sections (7μm) cut and mounted onto poly-l-lysine-coated glass slides (Sigma-Aldrich). Immunohistochemistry was performed as previously described using goat anti-gremlin antibody (R&D Systems)[3]. No staining was detected when gremlin primary antibody was omitted or substituted with an irrelevant antibody also raised in goat (anti-HAND1, R&D Systems).

Specimens from human lungs with IPAH (*n* = 2) and FPAH (*n* = 2) were obtained at time of transplant while control specimens were obtained from lung tissue resected during surgery for cancer at a site remote from the tumor margins. All patients had provided full written consent. Sections were prepared and immunostained for gremlin as above.

Immunoflourescence Staining

Mouse lungs were fully inflated using paraformaldehyde (1%) for 30mins and then placed into sucrose solutions (30%) at 4˚C for 24 hours before infiltration with OCT compound (Tissue Tek®, Sakura Finetek). Sections (10 microns) were cut and mounted onto poly-L-lysine coated slides for immunostaining and fluorescent labelling using the tyramide signal amplification (TSA™ Biotin System, Perkin Elmer Inc.). Slides were immersed in glycine (100mM) for 45 minutes to quench formaldehyde-induced fluorescence followed by immersion in sodium borohydride

(0.1%) for 30mins. Slides were washed and blocked in TNB blocking buffer (supplied in TSA™ kit) for 30mins, and incubated with anti-gremlin antibody (R&D Systems) overnight at 4°C. Slides were then incubated in biotinylated rabbit anti-goat secondary antibody (Vector Laboratories) for 1 hour, washed, and incubated in streptavidin-HRP (supplied in TSA™ kit) and subsequently biotinyl tyramide amplification reagent (supplied in TSA™ kit). FITC-streptavidin (Sigma-Aldrich) was added for 1 hour. Tissue sections were counterstained with 4',6-diamidino-2-phenylindole (Sigma-Aldrich) and mounted using Vectashield (Vector Laboratories). Images were acquired using a confocal laser-scanning microscope (Zeiss, LSM 510 Meta, x40/NA1.3 and x63/NA1.4 oil immersion objectives). No fluorescence was observed when gremlin primary antibody was omitted.

Western Blotting and ELISA

Western blot analysis was performed using whole lung and cell lysates that were lysed in radioimmuno-precipitation assay (RIPA) buffer supplemented with serine protease inhibitor, phenlyethanesulfonylflouride (PMSF), and a cocktail of protease and phosphatase inhibitors (Sigma-Aldrich). Tissue was homogenised (Ultra-Turrax T8, Carl Stuart) and cells were lysed by repetitive vortexing. Total protein content was determined using the bicinchoninic acid (BCA) assay (Pierce). Cell conditioned medium was concentrated using 5kDa Ultra-15 filters (Millipore) by centrifugation in a swinging bucket rotor (4000g for 45mins at 4°C). Protein extracts were separated by 15% (vol/vol) SDS-PAGE and blotted using: rabbit p-Smad1/5/8 (Cell Signaling Technology), rabbit total Smad1/5/8 (Santa Cruz Biotechnology), goat gremlin (R&D Systems), goat BMPR2 (R&D Systems), rabbit BMP2 and BMP4 (Abcam). These were detected with the respective, species-specific horseradish peroxidise-

conjugated secondary antibodies (Dako and Chemicon). Densitometry was performed using ImageJ software normalising to GAPDH or vehicle.

An Enzyme-Linked Immunosorbent Assay (ELISA) (R&D Systems) was used to examine the presence of secreted BMP ligands in concentrated conditioned medium from HMVEC-L. ELISAs were performed according to the protocols provided by the manufacturer (R&D Systems).

Cell Culture

For *in vitro* studies, primary human pulmonary microvascular endothelial cells from lung (HMVEC-L) and primary smooth muscle cells isolated from human pulmonary artery (PASMC) were bought in from Lonza Bioscience (formerly Cambrex). Cells were grown on sterile tissue culture dishes in Endothelial Growth Medium (EGM-2MV; Code: CC-3202) or Smooth Muscle Growth Medium (SmGM-2; Code CC-3182) according to the manufacturers instructions. All cells used in these experiments were passage 6-7 and were routinely checked for mycoplasma contamination using the VenorGeM PCR kit (Cambio Ltd). For hypoxic experiments, cells were placed in a hypoxic chamber (Coy Labs) and cultured in an atmosphere of 1% O_2, 5% CO_2 and 94% N_2 for 48 hours. Control conditions were achieved by culture in 21% O_2, 5% CO_2 and 74% N_2 in a cell-culture incubator.

To knock-down endogenous HIF1α or HIF2α, cells (HMVEC-L) were transfected with 10nM of a Smartpool HIF1α or HIF2α-specific siRNA respectively (Dharmacon) using lipofectin (Invitrogen Life Technologies). A non-targeting Smartpool siRNA was used as a negative control. Cells were grown on 6 well plates in EGM-2MV medium without antibiotics. When cells were 30-40% confluent, cells were transfected using Optimem reduced-serum media for 4 hours. Following

transfection cells were placed in normoxic or hypoxic (1% O_2) conditions for a further 48 hours. HIF1α and HIF2α mRNA expression levels were measured by Real-Time RT-PCR to confirm effective reduction with specific siRNA. Gremlin 1 expression was also analysed by Real-Time RT-PCR.

For Smad1/5/8 phosphorylation experiments hypoxic serum-free conditioned medium (CM) was taken off cells that were incubated in hypoxia for 48 hours and briefly centrifuged to remove dead cells. For detection of Smad1/5/8 phosphorylation, cells were serum-starved overnight in serum-free medium (SFM) containing supplements and treatments were added the following day for 1 hour as follows: 2 micrograms/ml of recombinant gremlin 1, 80ng/ml of BMP4 or 100ng/ml of BMP2 (all from R&D Systems). To block gremlin 1 antagonizing activity, 15 micrograms/ml of anti-gremlin antibody (R&D Systems) was pre-incubated with hypoxic conditioned medium or recombinant gremlin 1 for 1 hour prior to treatment. In all experiments in which hypoxia conditioned medium was not added unconditioned medium was added instead.

The concentrations of recombinant BMP2 (100ng/ml) and BMP4 (80mn/ml) used were chosen from within the range of concentrations previously reported[4-10]. In pilot experiments, we confirmed that the chosen concentrations accelerated wound healing compared to vehicle but did not cause complete wound closure; thus the effect of any further intervention, which *a priori* might either have reduced or augmented the effect of the BMPs, could be detected.

The concentration of recombinant gremlin used (2mg/ml) was selected based on previously published reports[11,12]. In pilot experiments we confirmed that this concentration blocked BMP2-induced Smad phosphorylation. We then confirmed that we had identified a concentration of gremlin that produced an inhibitory effect on

BMP2-induced Smad phosphorylation and endothelial wound healing similar to that of hypoxia conditioned medium. These findings suggest that the concentration of recombinant gremlin we used produced local concentrations of biologically active gremlin in the endothelial cell microenvironment similar to those produced by hypoxic endothelial cells.

For scratch healing assays HMVEC-L were seeded and allowed to grow to a confluent monolayer and a single vertical scratch was applied to each chamber using a 10-100 microlitre pipette tip (Greiner). Treatments were added in low-serum medium (3%) for 24 hours and percentage wound closure was measured using ImageJ software as previously described[3]. Hypoxia conditioned medium for these experiments was prepared as described above. In all experiments in which hypoxic conditioned medium was not added, unconditioned medium was added instead. Six fields of view in each well were measured at the pre-defined positions (above and below each drawn line) and each experiment was repeated six times.

Assessment of hypoxia-induced changes in pulmonary vascular resistance

Pulmonary hemodynamic responses were assessed using an isolated ventilated lung preparation perfused at constant flow, as previously described[13]. This preparation permits direct assessment of pulmonary vascular resistance independently of alterations in cardiovascular function, reflex, hormonal or other factors changed by chronic hypoxia[14-16]. Wild-type and grem1$^{+/-}$ mice were exposed to hypoxic (F_IO_2=0.10) conditions in a normobarbic environmental chamber or maintained in normoxia (F_IO_2=0.21) in the same room for 3 weeks, as previously described[15]. The hypoxic chamber was opened for 30 minutes every 1-2 days for

changes of water, feed and bedding and removal of mice from, or additon of mice to, the chamber.

Following exposure, mice were then anaesthetised (70mg.kg^{-1} sodium pentobarbitone (Rhône Merieux Ltd, Harlow, UK) intraperitoneally and anti-coagulated (1000 units kg^{-1} heparin). A cannula was then inserted into the trachea via tracheostomy and the mouse ventilated (5% CO_2 in air, tidal volume of 250µl, respiratory frequency 90). The femoral artery was then exposed and the mouse killed by exsanguination. A sample of blood was obtained for measurement of hematocrit. A midline incision was made through the sternum and the ribs retracted to expose the heart and lungs. A cannula was then inserted into the pulmonary artery and left atrium. The lungs were perfused (2ml/min) with DMEM heated to 37°C, pH 7.45 with Ficoll (4 g/100ml, PM 70, Sigma-Aldrich) according to standard protocols[13] and were hyperinflated to an airway pressure of 15cmH_2O every 5 minutes. End expiratory pressure was set to 1.6 mmHg and the venous outflow pressure to 2 mmHg. Following stabilization of the preparation, pressure measurements were recorded as the mean of 10 determinations made at end expiration during consecutive breaths, thus ensuring that vascular pressures and resistance were determined in Zone 3 conditions. Measurements were made in the final minute prior to a regular hyperinflation. In a subset of lungs, the rho kinase inhibitor Y27632 (Merck Biosciences) was then added to the perfusate (10^{-5}M) and vascular pressures recorded once the reductions had stabilized[15].

After completion of the perfusion protocol, the hearts were separated from the lungs, fixed by immersion in paraformaldehyde (4%) and stored. The atria were removed at the level of the atrioventricular junction in the plane of the mitral and tricuspid annuli i.e. at the level of the openings of the tricuspid and mitral valves

where the valve leaflets attach. The ventricles were then transected parallel to this plane at two levels, one third and two thirds of the distance from the atrioventricular junction to the apex of the heart. The relative cross sectional areas of the cut surfaces of the right and left ventricles were determined at each of these two levels and the mean of the two results was taken as the value for that heart (RV:LV+S). The cross sectional areas of the cut surfaces of the right and left ventricle were determined by stereological analysis. Images of the cut curfaces were acquired, digitised and viewed under a superimposed stereological grid showing regularly spaced points (Visiopharm integrator system version 2.9.11.0; Olympus Denmark). Points landing on right ventricle and on left ventricle+septum were separately counted and the ratio of these two determined at each level. The mean of these two values was taken as the RV:LV+S for that heart.

Stereological Quantification of Pulmonary Vascular structure

Hypoxia induced changes in pulmonary vascular structure were assessed in separate groups of wild-type and grem1$^{+/-}$ mice exposed to hypoxic or normoxic conditions for 3 weeks. Mice were then anaesthetized (sodium pentobarbitone 70mg.kg^{-1}, Rhône Merieux Ltd) intraperitoneally and anti-coagulated (1000 units kg^{-1} heparin). A midline incision was made through the sternum and the ribs retracted to expose the lungs. Tracheal and pulmonary arterial cannulae were inserted into the pulmonary artery as described above. An incision was made in the apex of the left ventricle to facilitate free drainage of perfusate. Initially rho-kinase inhibitor (Y-27632 10^{-5}M, Merck Biosciences) in normal saline was perfused through the pulmonary circulation to inhibit ROCK activity and ensure complete relaxation of vasomotor tone[15]. Defibrinated horse blood (Cruinn Diagnostics Ltd.) was then perfused

through the vasculature (pulmonary arterial pressure 30cmH_2O above the hilum) until the pulmonary vessels were uniformly filled. The presence of erthyrocytes in the vascular space facilitated identification of vessels within the pulmonary parenchyma following the preparation of sections for microscopic examination. Horse erythrocytes are of similar size (average diameter 5.8 microns) to mouse red blood cells (average diameter 6.1 microns)[17]. Once all the blood vessels had been filled, as indicated by a uniformly red appearance of all lung lobes, the wound at the apex of the left ventricle was closed using a vascular clamp ensuring that pressure throughout the vessels was uniform (30cmH_2O). The pulmonary arterial trunk was then tied closed using a ligature and the lungs were then fully inflated (pressure of 25 cm of water) by intratracheal instillation of glutaraldehyde (2.5% wt.vol^{-1}) for 30 minutes. The left main bronchus was then tied closed at the hilum so that the volume of air spaces, airways and vessels was maintained constant, the left lung then separated and immersed in fixative overnight.

Left lung volumes were measured by water displacement[18]. The left lung was then processed for stereological quantification of the pulmonary vascular bed[18, 19]. In brief, the lung was divided into multiple blocks from a random start point and blocks selected for embedding in araldite resin using a systematic randomized strategy. Tissue blocks were embedded in spherical moulds to ensure sectioning in isotropically uniformly random orientations. Semithin sections (1μm) were cut from each of the resin-embedded blocks and stained with toluidine blue.

Image analysis

Randomly acquired images (Olympus BX61 motorised microscope) of the tissue sections were digitized (Olympus DP70 digital camera) and displayed on screen to

permit superimposition of stereologic grids for analysis using a computer-assisted stereological toolbox (CAST) system (Visiopharm integrator system version 2.9.11.0; Olympus). All slides were identified by code so that the observer was blinded to the experimental conditions. Pulmonary vascular remodeling was assessed in the intra-acinar vessels. A counting frame with two inclusion and two exclusion boundaries (Supplemental Figure 1) was used to determine the length density of the vessels within the gas exchange region of the lung (intra-acinar vessels) and unbiased selection of vessels for direct measurement of lumen diameter. Using this strategy the probability of selection of a vessel for lumen diameter measurement was directly proportional to the total length of vessel within the lung in that diameter category[18]. The lumen diameter was taken as the maximum distance across the lumen measured perpendicular to a line drawn along the longest axis of the image of the transected lumen (Supplemental Figure 1). The external diameter of the vessels was measured at the same position as the lumen diameter. Wall thickness was calculated as half the difference between the external and internal (lumen) diameters. A point counting grid was also included that allowed determination of the volume fraction of the vascular lumen within the lung. Intra-acinar vessels were identified as those accompanying respiratory bronchioles or more distal airways and alveoli which had a lumen diameter greater than 10 microns and less than 50 microns.

Statistical Analyses

Normally distributed data are reported as means (±SEM) while non-normally distributed data are presented as medians ± inter quartile range (IQR). For normally distributed data, determination of the statistical significance of differences between two groups means in planned a priori comparisons were made using paired or

unpaired t-tests as appropriate. For non-normally distributed data statistical significance was determined using the Mann-Whitney U or Wilcoxon tests; p-values were computed using the exact (permutation) method. Multiple post hoc comparisons across experimental groups were made using the Holms-Sidak step-down test to correct for multiple comparisons[20]. Statistical analysis was undertaken using PASW 18 (formerly SPSS), IBM. Values of $P<0.05$ were accepted as statistically significant.

Supplemental Tables

Supplemental Table 1. Mean (±SEM) vessel length density in the lungs of the four experimental groups following three weeks of hypoxic exposure.

	Wild-type (grem1+/+)		**Haplodeficient (grem1+/-)**	
	Normoxia	Hypoxia	Normoxia	Hypoxia
Vessel length density ($cm.cm^{-3}$)	2461 (±151)	2024* (±110)	2390 (± 135)	2132 (± 104)

There was a significant decrease in pulmonary intra-acinar vessel density in the wild-type mice following long-term hypoxic exposure that was not observed in the $grem1^{+/-}$ haplodeficient mice. n=8 per group. * signifies significant differences from matched normoxic control, $P<0.05$.

Supplemental Table 2. The total increase in pulmonary vascular resistance (PVR), the vasoconstricor (Y-27632 reversible) component, the difference between these two and the calculated component caused by vascular remodeling (determined using Poiseuille's equation) in chronically hypoxic wild-type and haplodeficient ($grem1^{+/-}$) mouse lungs.

	Total PVR increase	**Constriction (Y-27632)**	**Difference**	**Remodelling (Poiseuille)**
Wild-type ($Grem1^{+/+}$)	0.85* (0.032)	0.37* (0.04)	0.47* (0.04)	0.54* (0.089)
$Grem1^{+/-}$	$0.63^{*\#}$ (0.043)	0.33* (0.03)	$0.32^{*\#}$ (0.04)	$0.27^{*\#}$ (0.14)

Values are means (±SEM). All values in chronically hypoxic mouse lungs are expressed normalised to the mean normoxic values. Total PVR increase was calculated as the measured increase in PVR in each chronically hypoxic lung divided by the mean normoxic PVR. The vasoconstrictor component was calculated as the reduction in PVR induced by Y27632 divided by the mean normoxic PVR. The difference between the total PVR and the Y27632-induced reduction was taken to approximate the component of the chronic hypoxia-induced increase that was caused by vascular remodelling. The predicted increase in PVR due to structural change was calculated based on the stereologically derived data on vascular structure. As the total length of vessels in the lung was unchanged following hypoxic exposure (Figure 7D), the structural component of the increase in PVR was caused solely by reduction in the radius of the lumen. Thus the change in the structural

component of the increase in PVR was modelled using Poiseuilles equation in which baseline vascular radius was taken to be the mean vessel radius in normoxic lungs. In both wild-type and haplodeficient mouse lungs the hemodynamically determined structural component of PVR (Difference) and the calculated structural component based on the measured changes in vascular structure are similar in magnitude. Furthermore, it can be seen that the reduction in chronic hypoxic PVR caused by gremlin haplodefidiency was entirely due to a reduction in the structural component of the hypoxia-induced increase. * indicates statistically significant difference from 0 i.e. normoxia (P<0.01). # indicates statistically significant difference from wild-type value (P<0.05).

Supplemental Figures and Figure Legends.

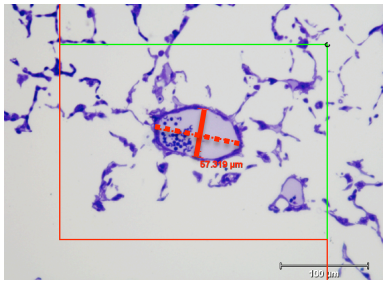

Supplemental Figure 1. Image showing method of stereological analysis of vessel lumen diameter and wall thickness - inclusion/exclusion frame. A counting frame was superimposed over randomly acquired images of lung tissue sections using CAST software. When the lumen of an intra-acinar vessel fell on the green line (inclusion line) or inside the frame it was counted and the internal and external diameters measured at a site perpendicular to the longest axis (dotted line). If the lumen of a vessel fell on the red line (exclusion line) it was excluded. x20 objective, scale bar represents 100μm.

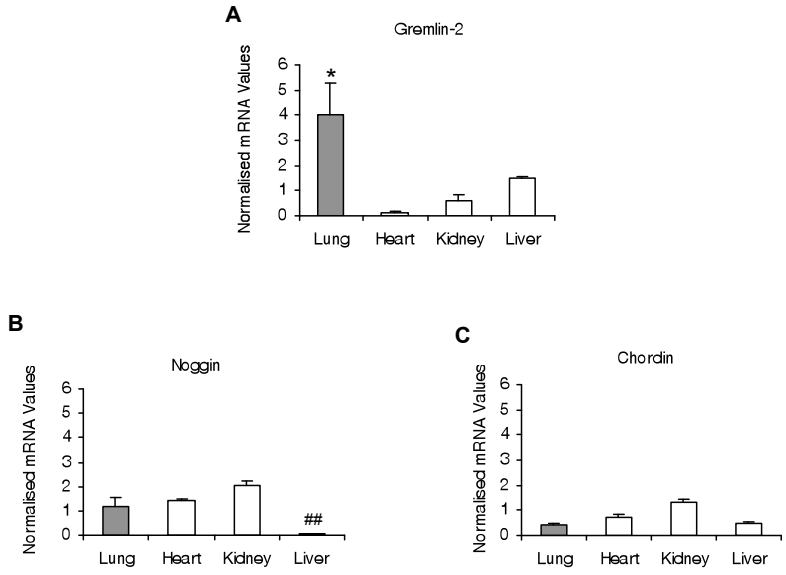

Supplemental Figure 2. High basal gremlin 2 (also known as protein related to dan and cerebrus, PRDC) expression in the lung. (**A**) The secreted BMP antagonist gremlin 2 (mean±SE), which is highly homologous to gremlin 1, was more highly expressed in the lung compared to the systemic organs. The other well characterized secreted BMP2 and BMP4 antagonists noggin (**B**) and chordin (**C**) did not show the disproportionately high expression levels shown by gremlin 1 and gremlin 2 (mean±SE) (*n*=7). Values are normalized to 18S RNA. * indicates significant difference from all other organs ($P<0.05$). ## indicates significant difference of liver from other organs ($P<0.01$).

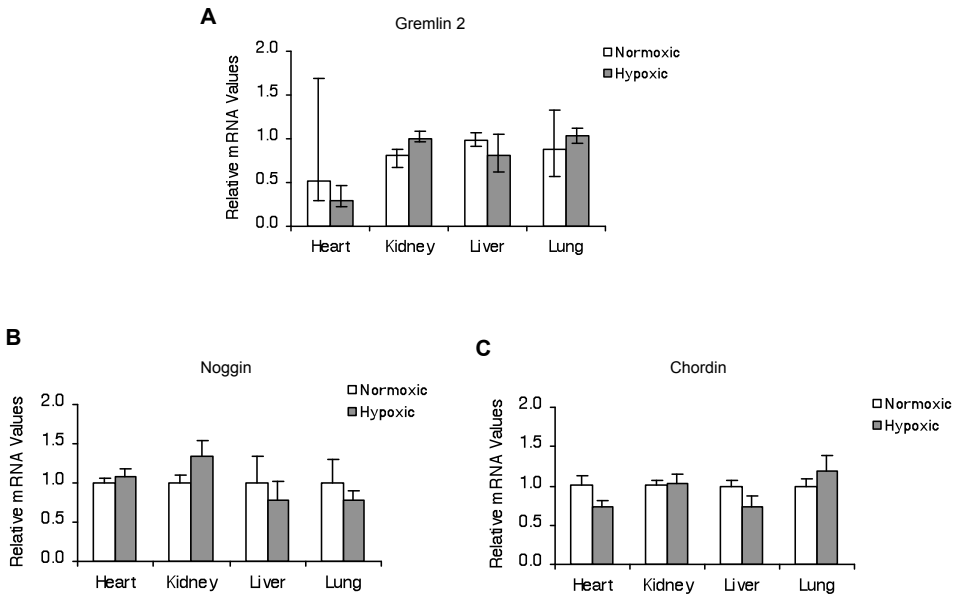

Supplemental Figure 3. The BMP antagonists gremlin 2, noggin and chordin were unaltered in response to hypoxia. (**A**) The secreted BMP antagonist gremlin 2 (median±IQR) which is highly homologous to gremlin 1 was not altered in response to two days of hypoxic exposure in any of the organs analyzed. Values are normalized to 18S RNA and expressed as fold-change relative to normoxic control for each organ. The other secreted BMP antagonists noggin (**B**) and chordin (**C**) also remained unchanged in response to hypoxia (mean±SE) (*n*=7). Values are normalized to 18S RNA and expressed as fold-change relative to normoxic control for each organ.

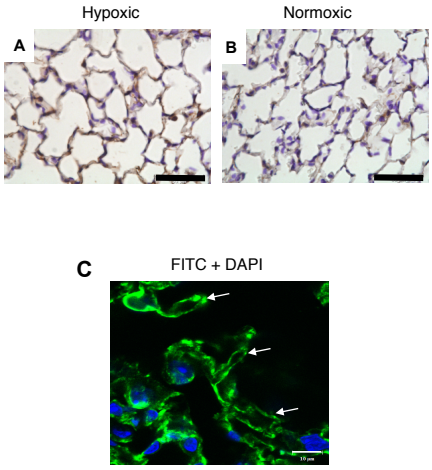

Supplemental Figure 4. Representative images showing gremlin within the alveolar wall. Immunohistochemical staining (brown) of gremlin in a mouse lung showed increased gremlin expression within the alveolar walls following 48 hours of hypoxic exposure (A) when compared to basal normoxic (B) conditions. (x40 objective). Scale bar represents 50μm. (C) Representative confocal image of immunofluorescent (FITC) staining of gremlin in sections from a normoxic mouse lung demonstrated that the labelling in the alveolar wall was observed in a pattern suggesting its localization predominantly in the capillary endothelium (x63 oil immersion objective). Scale bar represents 10 microns.

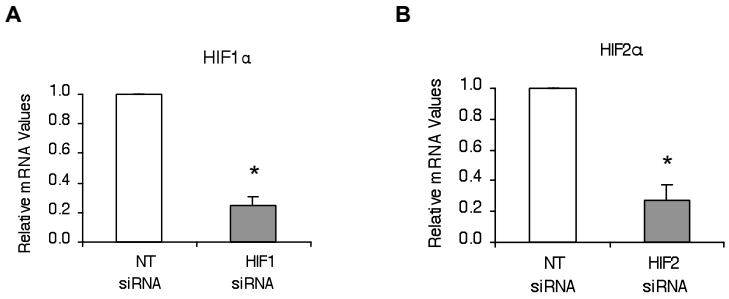

Supplemental Figure 5. Successful knockdown (mean±SE) of HIF1α and HIF2α by their respective targeting siRNA was confirmed by Real-Time PCR. Values (*n*=7 in each group) were normalised to 18S RNA and expressed as fold-change relative to the normoxic control mean (ctrl –siRNA).

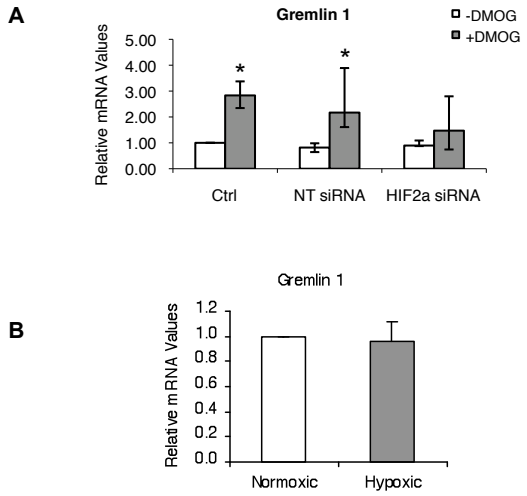

Supplemental Figure 6. (A) The prolyl hydroxylase inhibitor dimethyloxalylglycine (DMOG) induced increases in gremlin 1 expression in pulmonary endothelial cells that required HIF2a. Under control conditions in the absence of siRNA (Ctrl) and in the presence of non-targeting siRNA (NT siRNA), DMOG (10^{-3}M) caused significant increases in gremlin 1 expression (median±IQR). siRNA mediated knockdown of HIF2a blocked the DMOG induced response of gremlin (HIF2a siRNA). Note that in the absence of DMOG siRNA did not significantly alter gremlin expression (non-targeting and siRNA targeting HIF2a). Values are shown as medians ±inter quartile ranges (n=6-7 per group) * indicates significant difference from matched normoxic group ($P<0.05$, Wilcoxon signed rank). **(B)** Gremlin 1 expression in human pulmonary artery smooth muscle cells was not significantly altered by two days of hypoxic exposure. Gremlin 1 mRNA expression (mean±SE) in PASMCs in response to 48 hours hypoxic exposure (*n*=4). Values are normalised to 18S RNA and expressed as fold-change relative to normoxic control.

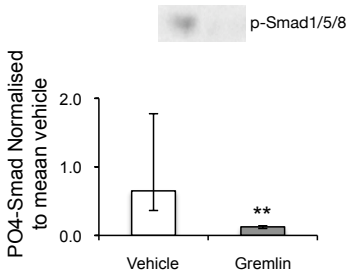

Supplemental Figure 7. Gremlin 1 inhibits basal Smad1/5/8 phosphorylation in human pulmonary microvascular endothelial cells. Treatment with recombinant gremlin 1 (2 micrograms/ml) for 1 hour significantly reduced basal Smad1/5/8 phosphorylation in these pulmonary endothelial cells. Densitometric analysis showed a statistically significant (***P*<0.01) reduction in Smad1/5/8 phosphorylation following gremlin 1 treatment (median±IQR). Values were normalized to vehicle control value (*n*=6).

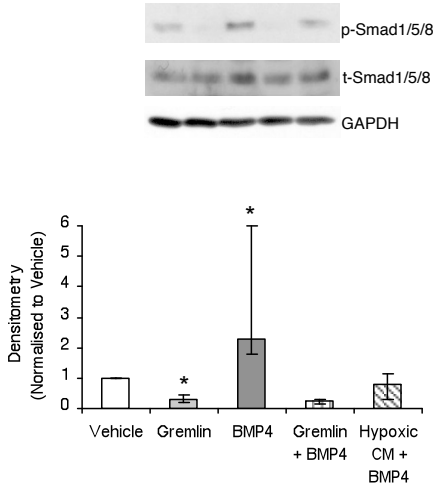

Supplemental Figure 8. BMP4 induces Smad1/5/8 in human pulmonary microvascular endothelial cells, which is similarly blocked by both recombinant gremlin 1 and hypoxia conditioned medium. Western blot showing Smad1/5/8 phosphorylation in pulmonary endothelial cells following treatment for one hour with vehicle, gremlin 1, recombinant BMP4, recombinant BMP4 together with recombinant gremlin 1, and BMP4 together with hypoxic conditioned medium respectively. Hypoxic conditioned medium was medium removed from pulmonary microvasclar endothelial cells that had been cultured in hypoxia for 48 hours. Densitometric analysis (median±IQR) showed that BMP4 treatment caused a significant increase in Smad1/5/8 phosphorylation whereas this action was not observed in the presence of gremlin 1 or hypoxia conditioned medium (*n*=6 per group). Gremlin 1 treatment alone reduced Smad1/5/8 phosphorylation significantly below that observed in the vehicle treated group. * and ** indicate significant difference from vehicle treatment ($P<0.05$ and <0.01 respectively).

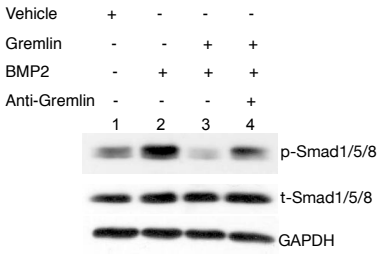

Supplemental Figure 9. Polyclonal goat anti-gremlin antibody blocks gremlin function. Western blot showing that BMP2 treatment for 1 hour induced Smad1/5/8 phosphorylation in human pulmonary microvascular endothelial cells (lane 2) that was blocked by recombinant gremlin 1 (lane 3). Anti-gremlin antibody prevented the inhibitory action of gremlin 1 on BMP2-induced Smad 1/5/8 phosphorylation (lane 4).

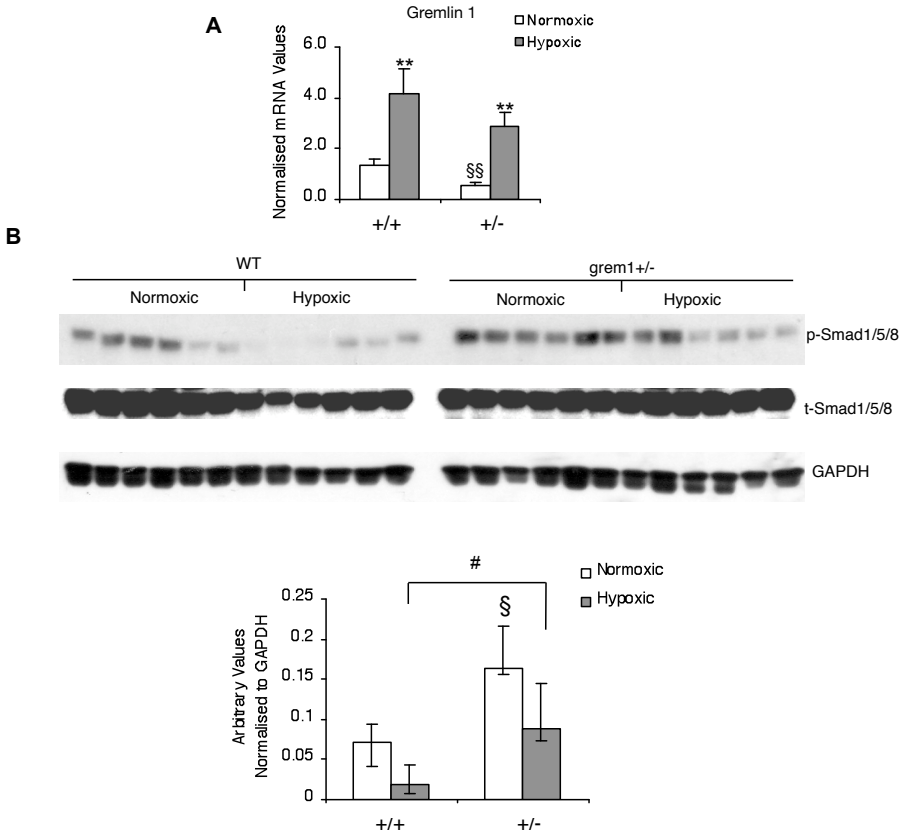

Supplemental Figure 10. Gremlin 1 expression and BMP signaling in grem1$^{+/-}$ and wild-type mice lungs. (**A**) Basal gremlin 1 mRNA expression (mean±SE) in grem1$^{+/-}$ is significantly less than that in wild-type mice lungs and is upregulated in response to 2 days of hypoxic exposure in both groups (*n*=8). (**B**) Smad1/5/8 phosphorylation (median±IQR) is higher in normoxic grem1$^{+/-}$ mice lungs than in normoxic wild-type mice lungs. Similarly Smad1/5/8 phosphorylation is higher in hypoxic grem1$^{+/-}$ mice lungs than in normoxic wild-type mice lungs (*n*=6). § indicates significant difference between normoxic wild-type and normoxic grem1$^{+/-}$ mice (P<0.05). # indicates significant difference between hypoxic wild-type and hypoxic grem1$^{+/-}$ mice (P<0.05).

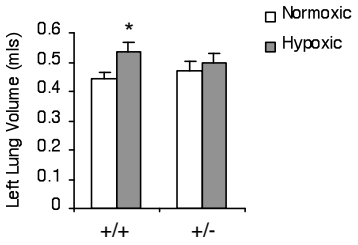

Supplemental Figure 11. The mean left lung volume (mean±SE) of the wild-type hypoxic mice was significantly larger than that of normoxic wild type mice. No significant difference was observed between the two grem1$^{+/-}$ groups. Thus, grem1$^{+/-}$ mice did not show the increased lung volume normally observed in response to chronic hypoxia [15, 21-23].

Supplemental References

1. Roxburgh SA, Kattla JJ, Curran SP, O'Meara YM, Pollock CA, Goldschmeding R, Godson C, Martin F, Brazil DP. Allelic Depletion of grem1 Attenuates Diabetic Kidney Disease. *Diabetes.* 2009;58(7):1641-1650.

2. Khokha MK, Hsu DR, Brunet LJ, Dionne MS, Harland RM. Gremlin is the BMP antagonist required for maintenance of Shh and Fgf signals during limb patterning. *Nat Genet.* 2003;34:303 - 307.

3. Costello CM, Howell K, Cahill E, McBryan J, Konigshoff M, Eickelberg O, Gaine S, Martin F, McLoughlin P. Lung-selective gene responses to alveolar hypoxia: potential role for the bone morphogenetic antagonist gremlin in pulmonary hypertension. *Am J Physiol Lung Cell Mol Physiol.* 2008;295(2):L272-284.

4. Kiyono M, Shibuya M. Inhibitory Smad transcription factors protect arterial endothelial cells from apoptosis induced by BMP4. *Oncogene.* 2006;25(54):7131-7137.

5. Star GP, Giovinazzo M, Langleben D. Effects of bone morphogenic proteins and transforming growth factor-beta on In-vitro production of endothelin-1 by human pulmonary microvascular endothelial cells. *Vascular Pharmacology.* 2009;50(1-2):45-50.

6. Zhang S, Fantozzi I, Tigno DD, Yi ES, Platoshyn O, Thistlethwaite PA, Kriett JM, Yung G, Rubin LJ, Yuan JXJ. Bone morphogenetic proteins induce apoptosis in human pulmonary vascular smooth muscle cells. *Am J Physiol Lung Cell Mol Physiol.* 2003;285(3):L740-754.

7. Rothhammer T, Bataille F, Spruss T, Eissner G, Bosserhoff AK. Functional implication of BMP4 expression on angiogenesis in malignant melanoma. *Oncogene.* 2006;26(28):4158-4170.

8. Maciel TT, Melo RS, Schor N, Campos AH. Gremlin promotes vascular smooth muscle cell proliferation and migration. *Journal of Molecular and Cellular Cardiology.* 2008;44(2):370-379.

9. Morrell NW, Yang X, Upton PD, Jourdan KB, Morgan N, Sheares KK, Trembath RC. Altered Growth Responses of Pulmonary Artery Smooth Muscle Cells From Patients With Primary Pulmonary Hypertension to Transforming Growth Factor-{beta}1 and Bone Morphogenetic Proteins. *Circulation.* 2001;104(7):790-795.

10. Suzuki Y, Montagne K, Nishihara A, Watabe T, Miyazono K. BMPs Promote Proliferation and Migration of Endothelial Cells via Stimulation of VEGF-A/VEGFR2 and Angiopoietin-1/Tie2 Signalling. *J Biochem.* 2008;143(2):199-206.

11. Mitola S, Ravelli C, Moroni E, Salvi V, Leali D, Ballmer-Hofer K, Zammataro L, Presta M. Gremlin is a novel agonist of the major proangiogenic receptor VEGFR2. *Blood.* 2011;116(18):3677-3680.

12. Wordinger RJ, Fleenor DL, Hellberg PE, Pang IH, Tovar TO, Zode GS, Fuller JA, Clark AF. Effects of TGF-beta2, BMP-4, and gremlin in the trabecular meshwork: implications for glaucoma. *Invest Ophthalmol Vis Sci.* 2007;48(3):1191-1200.

13. Weissmann N, Akkayagil E, Quanz K, Schermuly RT, Ghofrani HA, Fink L, Hanze J, Rose F, Seeger W, Grimminger F. Basic features of hypoxic

pulmonary vasoconstriction in mice. *Respir Physiol Neurobiol.* 2004;139(2):191-202.

14. Cadogan E, Hopkins N, Giles S, Bannigan JG, Moynihan J, McLoughlin P. Enhanced expression of inducible nitric oxide synthase without vasodilator effect in chronically infected lungs. *Am J Physiol Lung Cell Mol Physiol.* 1999;277(3):L616-627.

15. Hyvelin J-M, Howell K, Nichol A, Costello CM, Preston RJ, McLoughlin P. Inhibition of Rho-Kinase Attenuates Hypoxia-Induced Angiogenesis in the Pulmonary Circulation. *Circ Res.* 2005;97(2):185-191.

16. von Bethmann AN, Brasch F, Nusing R, Vogt K, Volk HD, Muller KM, Wendel A, Uhlig S. Hyperventilation induces release of cytokines from perfused mouse lung. *American journal of respiratory and critical care medicine.* 1998;157(1):263-272.

17. Perk K, Frei YF, Herz A. Osmotic Fragility of Red Blood Cells of Young and Mature Domestic and Laboratory Animals. *Am J Vet Res.* 1964;25:1241-1248.

18. Howell K, Costello CM, Sands M, Dooley I, McLoughlin P. L-Arginine promotes angiogenesis in the chronically hypoxic lung: a novel mechanism ameliorating pulmonary hypertension. *Am J Physiol Lung Cell Mol Physiol.* 2009;296(6):L1042-1050.

19. Howell K, Preston RJ, McLoughlin P. Chronic hypoxia causes angiogenesis in addition to remodelling in the adult rat pulmonary circulation. *The Journal of Physiology.* 2003;547(1):133-145.

20. Ludbrook J. Multiple comparison procedures updated. *Clinical and experimental pharmacology & physiology.* 1998;25(12):1032-1037.

21. Cunningham EL, Brody JS, Jain BP. Lung growth induced by hypoxia. *J Appl Physiol.* 1974;37(3):362-366.

22. Howell K, Preston RJ, McLoughlin P. Chronic hypoxia causes angiogenesis in addition to remodelling in the adult rat pulmonary circulation. *J Physiol.* 2003;547(Pt 1):133-145.

23. Rabinovitch M, Gamble W, Nadas AS, Miettinen OS, Reid L. Rat pulmonary circulation after chronic hypoxia: hemodynamic and structural features. *Am J Physiol.* 1979;236(6):H818-827.